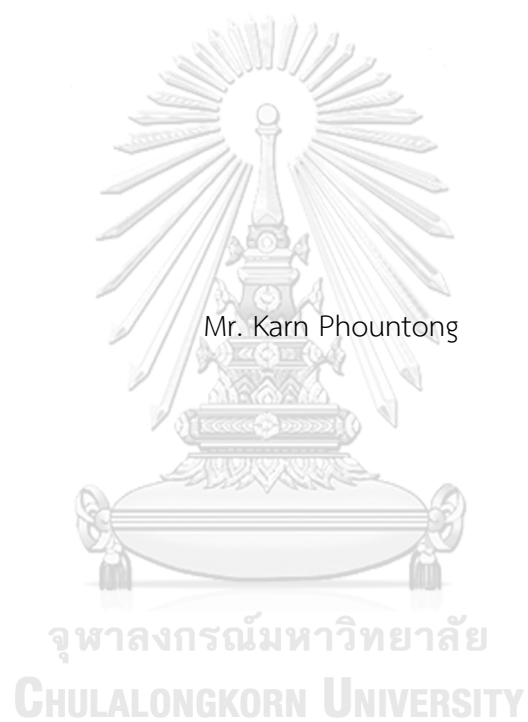GEOLOGICAL AND MINERALOGICAL CHARACTERISTICS OF PILOK AND TAKUA PIT
THONG TIN-TUNGSTEN DEPOSITS, WESTERN THAILAND

Mr. Karn Phountong

A Thesis Submitted in Partial Fulfillment of the Requirements

for the Degree of Master of Science in Geology

Department of Geology

FACULTY OF SCIENCE

Chulalongkorn University

Academic Year 2019

ลักษณะเฉพาะทางธรณีวิทยาและวิทยาแร่ของแหล่งแร่ดีบุก-ทังสเตนปิล็อกและตะกั่วปิดทอง ภาคตะวันตกของประเทศไทย

นายกาญจน์ เผื่อนทอง

จุฬาลงกรณ์มหาวิทยาลัย
CHULALONGKORN UNIVERSITY

วิทยานิพนธ์นี้เป็นส่วนหนึ่งของการศึกษาตามหลักสูตรปริญญาวิทยาศาสตรมหาบัณฑิต
สาขาวิชาธรณีวิทยา ภาควิชาธรณีวิทยา
คณะวิทยาศาสตร์ จุฬาลงกรณ์มหาวิทยาลัย
ปีการศึกษา 2562

Thesis Title	GEOLOGICAL AND MINERALOGICAL CHARACTERISTICS OF PILOK AND TAKUA PIT THONG TIN-TUNGSTEN DEPOSITS, WESTERN THAILAND
By	Mr. Karn Phountong
Field of Study	Geology
Thesis Advisor	ABHISIT SALAM, Ph.D.
Thesis Co Advisor	Takayuki Manaka, Ph.D.

Accepted by the FACULTY OF SCIENCE, Chulalongkorn University in Partial Fulfillment of the Requirement for the Master of Science

.... Dean of the FACULTY OF SCIENCE

(Professor POLKIT SANGVANICH, Ph.D.)

THESIS COMMITTEE

.... Chairman

(Assistant Professor VICHAI CHUTAKOSITKANON, Ph.D.)

.... Thesis Advisor

(ABHISIT SALAM, Ph.D.)

.... Thesis Co-Advisor

(Takayuki Manaka, Ph.D.)

.... Examiner

(Associate Professor PITSANUPONG KANJANAPAYONT, Dr.rer.nat.)

.... External Examiner

(Ladda Tangwattananukul, Ph.D.)

กาญจน์ เผื่อนทอง : ลักษณะเฉพาะทางธรณีวิทยาและวิทยาแร่ของแหล่งแร่ดีบุก-ทังสเตนปิล็อกและตะกั่วปิดทอง ภาคตะวันตกของประเทศไทย. (GEOLOGICAL AND MINERALOGICAL CHARACTERISTICS OF PILOK AND TAKUA PIT THONG TIN-TUNGSTEN DEPOSITS, WESTERN THAILAND) อ.ที่ปรึกษาหลัก : อ. ดร.อภิสิทธิ์ ซา ลำ, อ.ที่ปรึกษาร่วม : ดร.ทากายูกิ มานากะ

เหมืองปิล็อกและเหมืองตะกั่วปิดทองเป็นเหมืองดีบุก-ทังสเตนทั้งตั้งอยู่ในแนวหินแกรนิตตะวันตก ถึงแม้ว่าหินโผล่จากทั้งสองพื้นที่จะผุมาก แต่ผลการศึกษาศิลาวรรณาและธรณีเคมีสามารถแบ่งหินแกรนิตออกได้เป็น 2 หน่วยได้แก่ หินแกรนิตเนื้อดอกและหินแกรนิตเนื้อขนาดเดียวซึ่งแสดงลักษณะที่คล้ายกันมาก ยกเว้นแร่ทัวร์มาลีนที่พบได้แค่ในหินแกรนิตเนื้อขนาดเดียวและเนื้อหินที่ต่างกันของหินทั้งสอง ข้อมูลธรณีเคมียังระบุหินแกรนิตเนื้อดอกว่าเป็นหินเฟอร์โรถึงแม็กนีเซียน แอลคาลิก เพอร์อะลูมินัส ในขณะที่หินแกรนิตเนื้อขนาดเดียวเป็นหินเฟอร์โรถึงแม็กนีเซียน แอลคาลิกถึงแอลคาไลแคลซิก เพอร์อะลูมินัส หินทั้งสองเป็นหินแกรนิตชนิดเอส นอกจากนี้แนวโน้มของธาตุหายากยังแสดงให้เห็นความสมบูรณ์ของธาตุลิโทไฟล์ที่มีขนาดไอออนใหญ่ (เช่น โพแทสเซียม รูบิเดียม) และธาตุลิโทไฟล์ที่มีประจุสูง (เช่น ไนโอเบียม แทนทาลัม) ข้อมูลข้างต้นสามารถสรุปได้ว่าหินแกรนิตทั้งสองเกิดจากการหลอมละลายบางส่วนในช่วงท้ายของหินตะกอน มีการผสมกันของเปลือกโลกตอนล่างที่มากกว่าและเนื้อโลกตอนบน ซึ่งเป็นผลมาจากเหตุการณ์ช่วงท้ายของการชนกันของแผ่นเปลือกโลกพื้นทวีป

สาขาวิชา	ธรณีวิทยา	ลายมือชื่อนิสิต ....
ปีการศึกษา	2562	ลายมือชื่อ อ.ที่ปรึกษาหลัก ....
		ลายมือชื่อ อ.ที่ปรึกษาร่วม ....

6072019523 : MAJOR GEOLOGY

KEYWORD: Granite, Pilok, Takua Pit Thong, Tin, Geochemistry

Karn Phountong : GEOLOGICAL AND MINERALOGICAL CHARACTERISTICS OF PILOK AND TAKUA PIT THONG TIN-TUNGSTEN DEPOSITS, WESTERN THAILAND. Advisor: ABHISIT SALAM, Ph.D. Co-advisor: Takayuki Manaka, Ph.D.

Pilok and Takua Pit Thong mine were one of tin-tungsten mines associated with the Western Granitoid Belt. Despite the very poor condition of the outcrop, petrographic and geochemical studies reveal two granitoid units: porphyritic granite and equigranular granite, which show similar petrography characteristics except for tourmaline that appears only in equigranular granite, and their textures. Based on whole-rock geochemistry, porphyritic granite is ferroan to magnesian, alkalic, peraluminous granite whereas equigranular granite is ferroan to magnesian, alkali to alkali-calcic, peraluminous granite. Both granites show S-type affinity. The REE patterns show enrichment in LILE (e.g. K, Rb) and HFSE (e.g. Nb, Ta). All above data indicate that both granites formed in the late stage of partial melting of sedimentary rock where larger portion of the lower crust were mix with the smaller portion of the upper mantle, resulting from the post-collision event of continental crusts.

Field of Study:	Geology	Student's Signature ....
Academic Year:	2019	Advisor's Signature ....
		Co-advisor's Signature ....

ACKNOWLEDGEMENTS

TABLE OF CONTENTS

Page

LIST OF TABLES

LIST OF FIGURES

จุฬาลงกรณ์มหาวิทยาลัย
CHULALONGKORN UNIVERSITY

CHAPTER I

INTRODUCTION

Preface

Tin is a soft metal with low melting point. It cannot be corroded by acid or oxidized by air. Also, since it is non-toxic and can be molten with other metal into an alloy, tin has been used all around the world as food container, soldering iron, etc. The biggest tin deposit area is located in Southeast Asia, called the Southeast Asian tin belt. Tin reserve in Southeast Asia is about 9.6 Megatons, 54% of world tin production (Schwartz et al., 1995). In early 1980s, tin annual production in Thailand had gone up to approximately 30,000 tons (The Industrial Technology Research Institute [ITRI], 2016). However, since the tin-price crisis in 1985, tin became almost priceless metal and most of tin mines were shutdown. Although it was once priceless, now, its value is rising. As a result, several investors are starting the exploration. Problem is, since a tin-price crisis, all work and research on tin and its deposit was suspended. Although Thailand possess one of the biggest tin resources of the world, but there is little new work or research on tin have been published after the tin price crisis.

Pilok tin-tungsten deposit in Kanchanaburi Province and Takua Pit Thong tin-tungsten deposit in Ratchaburi Province are both primary deposits which are associated with the Western Granite Belt of Southeast Asia (Mahawat, 1988; Lehmann et al., 1994). This granite belt is a north-south trend extending from Yunnan in China, Myanmar, Western Thailand, Upper Southern Thailand, and west of Sumatra island (Figure 1). Because Pilok and Takua Pit Thong are very well-known tin-tungsten deposits in Western Thailand, a study in these areas would represents typical tin-tungsten deposit in this granite belt.

Figure 1 A regional map (ERSI, 2009) showing locations of the study areas (pink circle) in Western Thailand. A dash line showing Southeast Asian granite belt boundaries (Charusiri et al., 1993).

Objective and Scope of Study

This thesis aims to study geological and mineralogical characteristics of Pilok and Takua Pit Thong tin-tungsten deposits and compare the study between these two deposits. The study involves field investigation, petrography, and whole-rock geochemistry of the granitic rocks in both areas. Mineralization study includes paragenetic sequence of ore and gangue minerals from both deposits and mineral chemistry of feldspar and tourmaline.

Location and Accessibility

Pilok and Takua Pit Thong tin-tungsten deposits are located in Western Thailand: Kanchanaburi Province and Ratchaburi Province, respectively (Figure 1). These provinces, which are adjacent to each other, are located in the lower Western Thailand where Three pagoda fault is the boundary in the north, and Tanao Si Mountain range in the west, between Thailand and Myanmar (Department of Mineral Resources [DMR], 2014).

1. Pilok tin-tungsten deposit

Pilok deposit is located approximately at 14° 40'N 98° 22'E in Ban E-Tong, Pilok Sub-district, Thong Pha Phum District, Kanchanaburi Province (Figure 2). From Bangkok, highway number 4 is taken to Nakhon Pathom Province. Then, take route number 323 to Thong Pha Phum District. After that, route 3272 is taken to reach Pilok Sub-district. Geographically, the deposit is located directly on Tanao Si Mountain Range and very close to the border between Thailand and Myanmar. As a result, the geography of the area is mountainous and has a lot of hills, cliffs, and waterfalls.

2. Takua Pit Thong tin-tungsten deposit

This deposit is located approximately at 13° 40'N 99° 10'E in Suan Phueng District, Ratchaburi Province, which is in the southeast of Pilok area (Figure 2). From Bangkok, highway number 4 is taken to Ratchaburi Province. Then, route 3087 is taken to reach Suan Phueng District. Finally, a small rural road is taken to reach the mine. Geographically, the area is also located directly on Tanao Si Mountain Range. As a result, the area is mountainous and has a lot of hills and cliffs.
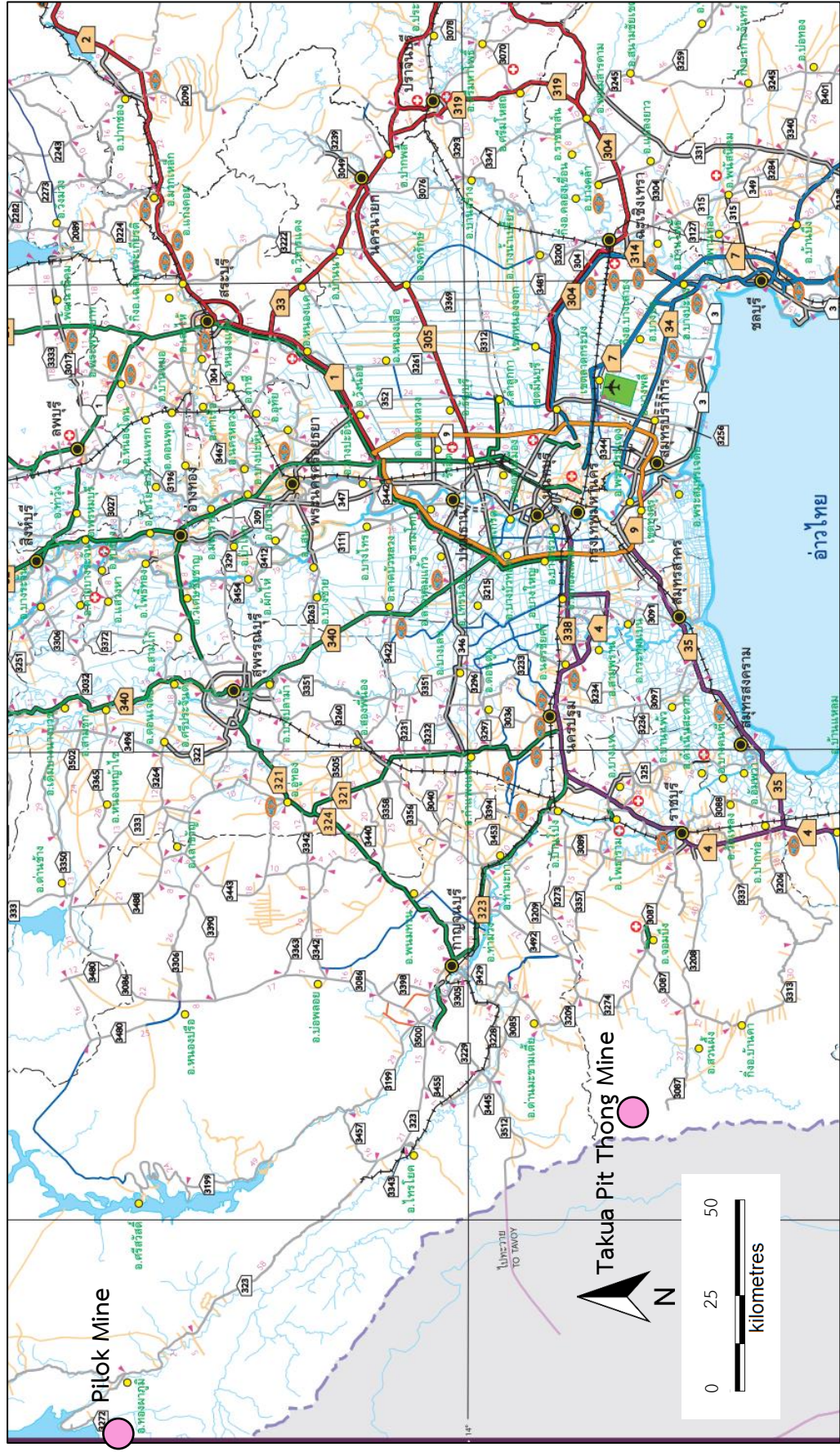
Figure 2 A highway map showing location and accessibility of the study areas (modified after Department of Highway, 2009).

Methodology

There are mainly 7 processes in this study, as illustrated in Figure 3. These processes are as followed:

1. <u>Fieldwork</u>

Fieldwork was divided into 2 phases: phase I at Pilok deposit and phase II at Takua Pit Thong deposit. Both phases had the same purpose, which is to gather information on field geological information and sampling for further analysis. The mining sites of both areas were the focus of field observation and sampling, especially granitic rocks, and ore-bearing quartz veins. Furthermore, field investigation has also been extended to the surrounding mines areas.

```
┌──────────────┐
│  Literature  │
│    Review    │
└──────┬───────┘
       ▼
┌──────────────┐
│  Fieldwork   │
└──────┬───────┘
       ▼
┌──────────────┐
│   Sample     │
│ preparation  │
└──────────────┘
```

Thin section, Polished-thin section

Rock powder

| Polarized light microscope | ⇔ | Petrography | | Major & minor Oxides | ⇔ | XRF |

| EPMA | ⇔ | Mineral Chemistry | | Trace element & REE | ⇔ | ICP-MS |

Discussion & Conclusion

Presentation & Thesis Writing
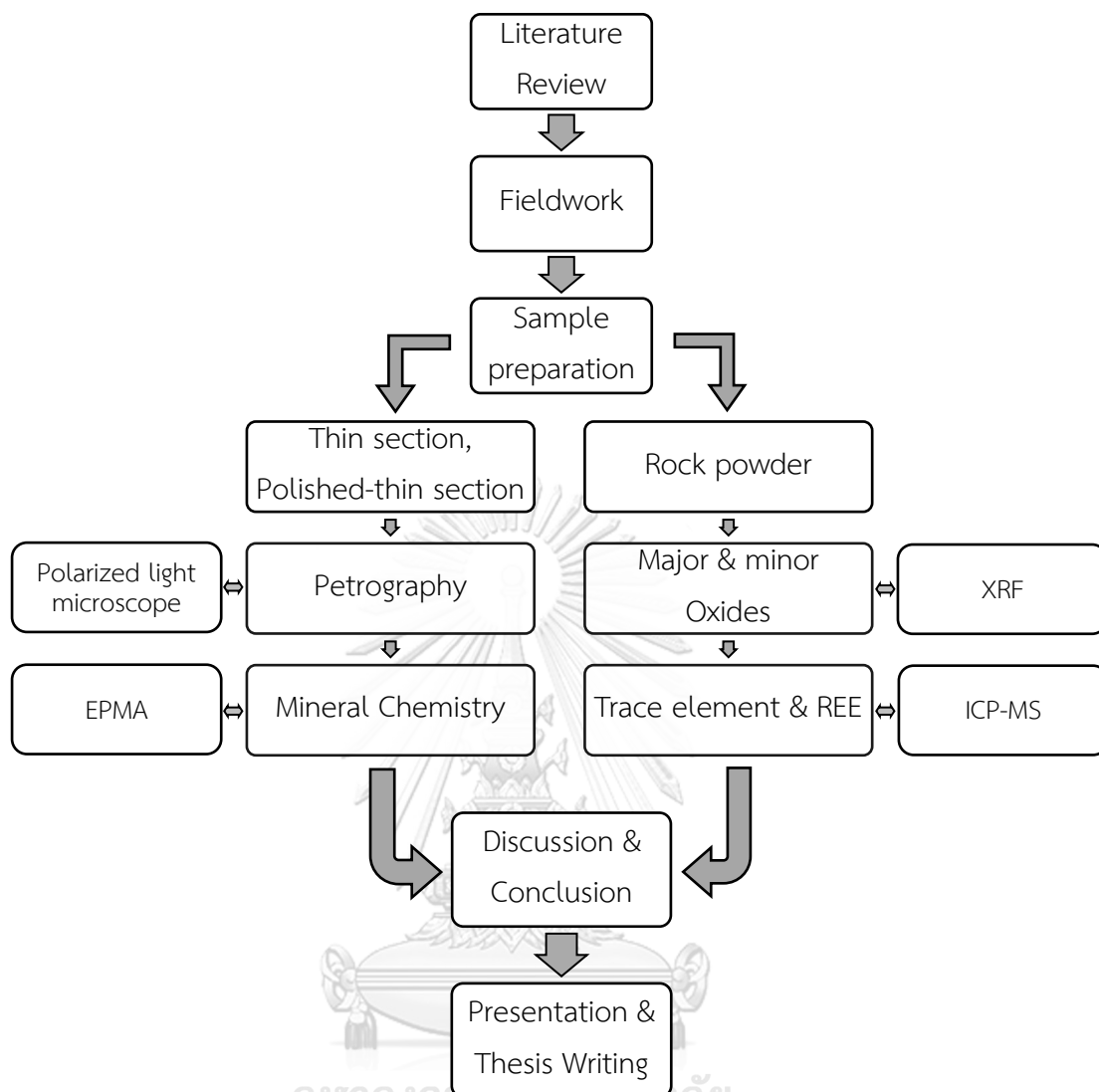
Figure 3 Methodology flow chart

2. <u>Sample preparation</u>

Various types of samples preparation had been undertaken at Department of Geology, Faculty of Science, Chulalongkorn University, as followed:

2.1. Thin section and polished-thin section

Firstly, samples were cut into slabs and grinded until the surface is flat. Then, slabs would be mounted on slides with balsam, or a mixture of epoxy and hardener to prepared a polished-thin section, and were grinded with 600-grit and 1200-grit silicon carbide, respectively, until it is 0.03 mm thick, or 0.08 mm if a polished-thin section was being prepared. Next, an amount of balsam was added to a thin section to attach a cover glass. But, if it was a polished-thin section we were preparing, it would be polished by hand using 9 μm, 6 μm, 3 μm, and 1 μm diamond paste, subsequently, until the surface is perfectly flat and smooth.

2.2. Rock powder

Selected samples were cut or smash by a rock hammer until they were approximately 5 – 10 cm long and crushed using a jaw crusher to turn them into 1 – 2 cm long rock chips. Since the jaw crusher often get contaminated from other samples, rock chips were washed and rinsed using distilled water and dried overnight. Then, cleaned rock chips were prepared using coning and quartering method (Horwitz, 1990), to cone them like a flat cake, divide them into four portions, and take the opposing two portion, to eliminate the heterogenous effect. After that, chips were grinded using a tungsten carbine disc mill until they are clay-size powder.

3. <u>Petrography</u>

Petrographic study aimed at describing petrography characteristics, particularly the mineral assemblage, texture, and the mutual relationship between minerals, of granitic rocks and other host rocks. Thin sections and polished-thin sections were studied using NIKON ECLIPSE LV100POL polarizing microscope at Department of Geology, Faculty of Science, Chulalongkorn University, both transmitted and reflected light. Furthermore, suitable mineral grains were selected for mineral chemistry analysis

4. Mineral Chemistry

Selected mineral grains were analyzed by JEOL model JXA 8100 Electron Probe Micro Analyzer (EPMA) at Department of Geology, Faculty of Science, Chulalongkorn University. The operating condition was 15.0 kV accelerating voltage with 25.0 nA current, and 1 μm beam size. However, tourmaline cannot be analyzed for some light elements, i.e. B, Li, H, and X-cite vacancy, by EPMA, thus, the estimation of these light elements had to be made. B^{3+} was estimated on the assumption that B^{3+} fully and only occupies the triangular B site (Henry, Viator, and Dutrow, 2002; Henry et al., 2011). Li^+ was estimated on the assumption that Li^+ fills any Y site deficiency (Henry et al., 2011). H^+ was estimated by charge balance after Li was estimated (Henry et al., 2011).

5. Major and minor oxides

This process was to study the whole-rock geochemistry of each unit of granitic rocks using X-Ray Fluorescence (XRF). After atoms were attacked by X-ray, they will be in an excited state and release energy as secondary X-ray called fluorescence, which is a characteristic feature of each element. The XRF machine used in this study was BRUKER model S4 PIONEER WDXRF (Wavelength Dispersive XRF) by Department of Geology, Faculty of Science, Chulalongkorn University. 8.000 g rock powder of each sample was mix with 1.000 g wax powder and pressed into a pellet. After introducing the pellet into the machine, major and minor oxides, including SiO_2, Al_2O_3, FeO_{total}, Na_2O, K_2O, MgO, CaO, TiO_2, MnO, and P_2O_5, were measured and calibrated with rock reference standard samples by United States Geological Survey (USGS) and Geological Survey of Japan (GSJ), i.e. RGM-1, GSP-2, AGV-2, BHVO-2, BCR-2, SDO-1, SGR-1, JG-2, JG-1a, JB-1b, and JCFA-1. In addition, loss on ignition (LOI) were analyzed by weigh rock powder samples before and after heating at 1000° C for 1 hour, as suggested by Lechler and Desilets (1987).

6. Trace element and rare earth element

This process was also to study the whole-rock geochemistry of each units of granitic rocks using Inductively Coupled Plasma Mass Spectrometry (ICP-MS). ICP-MS is a method using inductively coupled plasma as a medium to analyze samples by a

mass spectrometer, which separate atoms using its mass-charge ratio (m/q). Rock powder samples were sent to Australian Laboratory Service (ALS) Company Limited at Queensland, Australia, where they were fused with lithium borate and digest with various acid prior to the analysis. 31 elements, i.e. Ba, Ce, Cr, Cs, Dy, Er, Eu, Ga, Gd, Hf, Ho, La, Lu, Nb, Nd, Pr, Rb, Sm, Sn, Sr, Ta, Tb, Th, Tm, and U, were analyzed, calibrated, and report back to the author.

7. Discussion, conclusion, and thesis writing

Geochemical data and diagrams were processed and created by GCDkit Software (Janoušek, Farrow, and Erban, 2006). After all the analyses were complete, their data were integrated to discuss and conclude the geological and mineralogical characteristic of the study area.

CHAPTER II
LITERATURE REVIEW

Tectonic Setting

Sundaland, in which Thailand is located, is a combination of several continental blocks, volcanic arcs, and suture zones in between which represent oceans in the past (Metcalfe, 2017). These oceans were named after the timing of its existence: Paleo-Tethys in Devonian to Triassic; Meso-Tethys in Permian to Cretaceous; and Ceno-Tethys in Jurassic to Cretaceous (Ueno and Hisada, 1999; Metcalfe, 2011, 2013; Khin Zaw et al., 2014; Metcalfe, 2017). Thailand and parts of neighboring countries, i.e. Southern China (Yunnan), Myanmar, Laos, Vietnam, Cambodia, Peninsular Malaysia, and Eastern Sumatra Island of Indonesia, are believed to be comprised of three major continental terranes: Indochina Terranes in the east (Bunopas, 1981), Sibumasu Terrane (Metcalfe, 1984), which the northern part was known as Shan-Thai Terrane (Bunopas, 1981), with Sukhothai Arc (Barr and Macdonald, 1991) laying on the eastern edge of Shan-Thai Terrane and Loei Fold Belt (Bunopas, 1981) on the western edge of Indochina Terrane, and Western Myanmar Terrane in the west (Bunopas, 1981; Bunopas and Vella, 1983; Charusiri et al., 2002; Metcalfe, 2002, 2011; Khin Zaw et al., 2014; Metcalfe, 2017) (Figure 4). These three major terranes are originated from Australian part of Gondwanaland (Metcalfe, 1988; Barr and Macdonald, 1991; Charusiri et al., 2002; Khin Zaw et al., 2014)

Sibumasu Terrane is a north-south elongate terrane, covering Shan State and the peninsular of Myanmar; Northwest, Western, and Southern Thailand; Western Peninsular Malaysia, and Sumatra. It is bounded in the west and the southwest by Sagaing Fault, Mogok Metamorphic belt, Andaman Sea, and Medial Sumatra Tectonic zone (Barber and Crow, 2009), and in the east and the northeast by Inthanon Suture Zone (Barr and Macdonald, 1991; Sone and Metcalfe, 2008). In addition, it is considered to extend to the north into Baoshan Terrane (e.g. Ueno, 2003; Metcalfe, 2017) and probably Tengchong Terrane in Western Yunnan (Şengör, 1979; Metcalfe, 1984; Şengör, 1984; Metcalfe, 1988, 2002; Shi et al., 2008) or even to Qiangtang Terrane in Tibet (Metcalfe, 2017). Sibumasu Terrane is thought to be originated from

Northwestern Australian due many reasons. First evidence is the similarity of Cambrian to Lower Permian faunas and floras (Archbold et al., 1982; Burrett and Stait, 1985; Metcalfe, 1988; Burrett, Long, and Stait, 1990; Metcalfe, 1991, 1994, 2002; Wang et al., 2013). Second evidence is the presence of Upper Carboniferous to Lower Permian glaciomarine diamictites (Metcalfe, 1988; Stauffer and Lee, 1989; Ampaiwan, Hisada, and Charusiri, 2009; Chaodumrong, 2010; Ueno and Charoentitirat, 2011; Burrett et al., 2014). Third evidence is Lower Permian cool-water fauna and $\delta^{18}O$ cool-water indicators (Ingavat and Douglass, 1981; Waterhouse, 1982; Fang and Yang, 1991). Final evidence is Paleozoic paleomagnetic data suggesting the same southern paleolatitudes in Devonian, Carboniferous, and Permian of these two terranes (Bunopas, 1981; Metcalfe, 1988; Bunopas and Vella, 1989; Fang, Van der Voo, and Liang, 1989; Huang and Opdyke, 1991; Charusiri et al., 2002; Ali et al., 2013). Sibumasu Terrane was separated away from Gondwana in late Early Permian and collided with Sukhothai Terrane and Indochina Terrane in Middle to Late Triassic (Metcalfe, 2017). It has a Proterozoic basement of high-grade metamorphosed core complex with a wide range composition, i.e. para- and ortho gneiss, marble, calc-silicates, schist, and quartzite (Charusiri et al., 2002; Metcalfe, 2017). This is overlain by middle Cambrian to Early Ordovician siliciclastic rock: Tarutao Group in Thailand (Javanaphet, 1969; Metcalfe, 2017); Machinchang and Jerai Formations in Peninsular Malaysia (Jones, 1968), followed by middle and upper Paleozoic and Triassic shallow marine continental margin sedimentary rock and hemi-pelagic continental margin/slope sedimentary rock (Brown et al., 1951; Charusiri et al., 2002; Metcalfe, 2017).

Between these terranes, there are sutures in between, from west to east: Shan Boundary tectonic zone along Sagaing Fault and Mogok Metamorphic Belt, representing Meso-Tethyhs between Western Myanmar Terrane and Sibumasu Terrane (Charusiri et al., 2002; Metcalfe, 2017); Inthanon Suture Zone representing Paleo-Tethys between Sibumasu and Sukhothai Terrane (Sone and Metcalfe, 2008); Jinghong-Nan-Sra Kaeo Suture between Sukhothai Terrane and Loei Fold Belt, representing the collapsed back-arc basin (Sone and Metcalfe, 2008);.
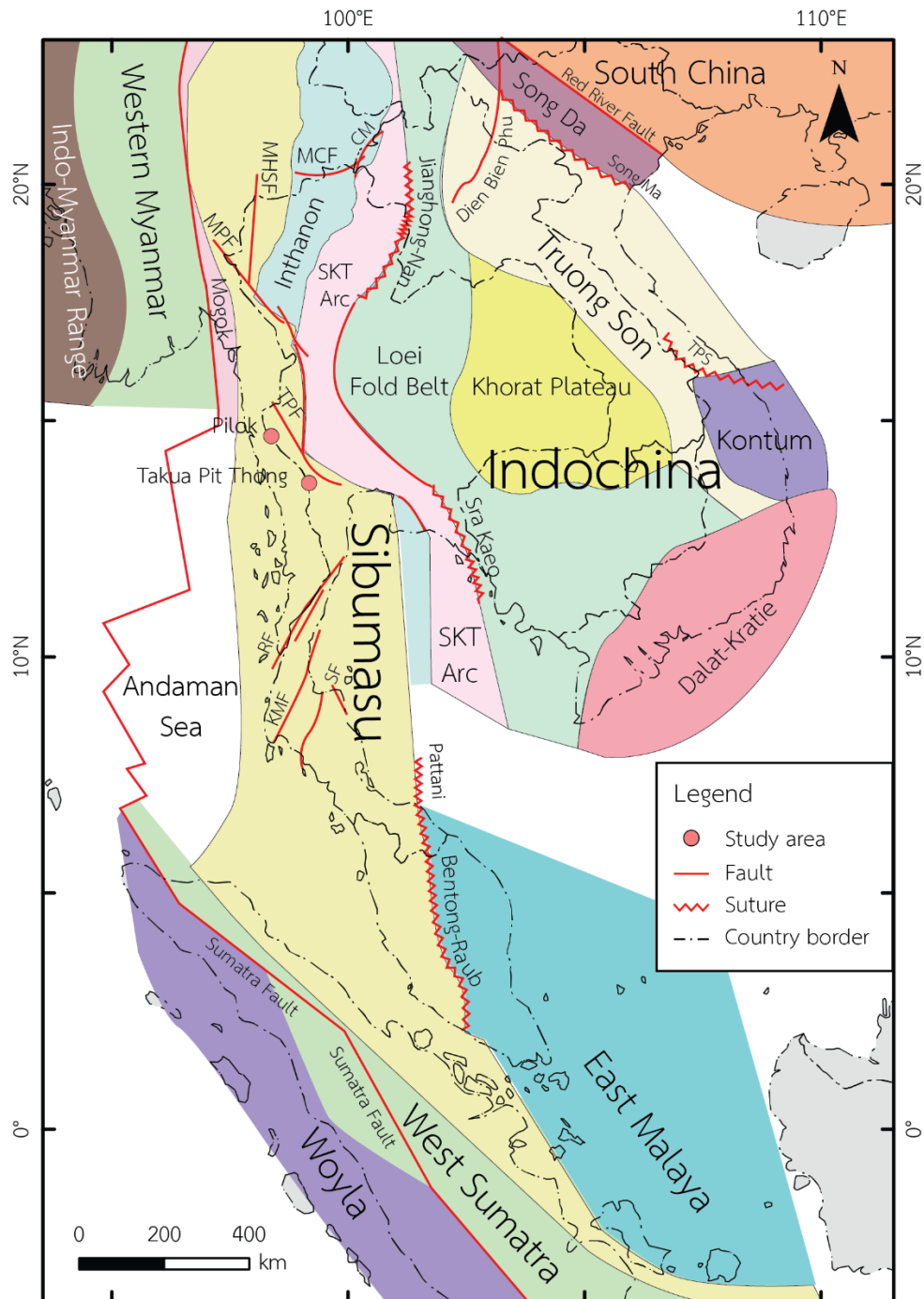
Figure 4 Mainland Southeast Asian tectonic map showing major terranes (distinguished by color) and major fault or sutures (modified after Charusiri et al., 2002; Sone and Metcalfe, 2008; Burrett et al., 2014; Khin Zaw et al., 2014; Metcalfe, 2017). Abbreviations: SKT = Sukhothai Arc; MCF=Mae Chan Fault, MHSF = Mae Hong Son Fault; MGF = Mae Ping Fault; TPF = Three Pagoda Fault; RF = Ranong Fault; KMF = Khlong Marui Fault; SF = Suraat Thani Fault; TPS = Tamky-Phuoc Son Suture; CM = Chiang Mai Suture.

Southeast Asian Granite Belt

There are three major granite belts in Thailand (Figure 5): The Eastern Granite Belt; The Central Granite Belt; and The Western Granite Belt (Cobbing et al., 1986; Cobbing et al., 1992; Charusiri et al., 1993). These three granite belts are also extended to Yunnan, Southern China, in the north (Sone and Metcalfe, 2008) which are called Yunxian-Jinggu Granite Belt in the east, Changning-Menglian Granite Belt in the middle, and Tengchong-Baoshan Granite Belt in the west (Wang et al., 2014).

The Eastern Granite Belt extended from Southern China, Northern Laos, Eastern Thailand along the Khorat Plateau, Eastern Peninsular Malaysia, Billiton Island, and Indonesia (Charusiri et al., 1993; Wang et al., 2014). The country rocks where this granite intruded are mostly Upper Paleozoic sedimentary rocks and volcaniclastic rocks (Charusiri et al., 1993). The belt can be further divided into three sub-belt, from east to west, East Coast Subprovince, Boundary Range Subprovince, and Central Subprovince of Hutchison (1977) (Schwartz et al., 1995). Evidence from whole-rock geochemistry indicated that this granite belt have characteristics of I-type granites (Cobbing et al., 1986; Charusiri et al., 1993; Schwartz et al., 1995). The extended Eastern Granite Belt in the north, Yunxian-Jinggu Granite Belt, also has the same properties as the Eastern Granite Belt in Thailand (Wang et al., 2014). There are many works on geochronology on these granites. Initially, Rb-Sr dating from the East Coast Belt and the Boundary Range Belt, which are included in the Eastern Granite Province, defines age of 220 to 263 Ma and 197 to 257 Ma respectively (Schwartz et al., 1995). Later, granites from 3 locations were dated by $^{40}Ar/^{39}Ar$ technique and were found to range from 245 to 210 Ma or Middle to Late Triassic (Charusiri et al., 1993). Afterwards, evidence from U-Pb zircons dating technique defines age of granite in Yunxian-Jinggu Granite Belt of 298 to 262 Ma or early Permian to middle Permian (Yu et al., 2003; Hennig et al., 2009; Li et al., 2011) and 239 to 189 Ma or late Middle Triassic to middle Early Jurassic (Bureau of Geology and Mineral Resources of Yunnan [BGMRY], Shi et al., 1989; 1990; Qin, 1991).
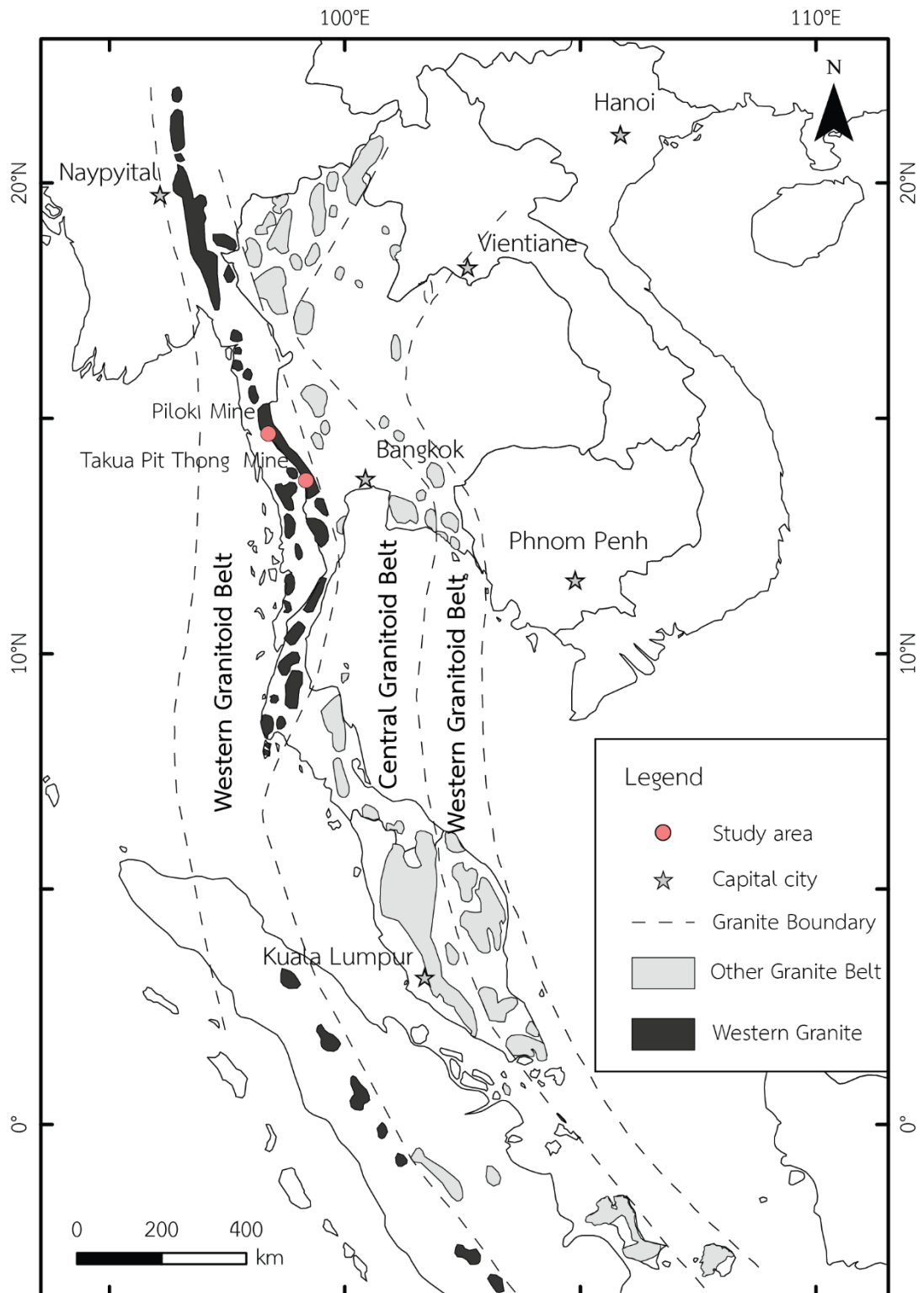
Figure 5   Granite distribution and Southeast Asian granite belt boundaries (modified after Charusiri et al., 1993)

The Central Granite Belt extended from Southern China, Central, and Northern Thailand, main range Peninsular Malaysia, Lower Peninsular, Bangka, Singkep, and Tuju Islands of Indonesia (Charusiri et al., 1993; Wang et al., 2014). The country rocks where this granite intruded are Late Paleozoic to Early Mesozoic clastic sedimentary rocks without any volcanic or volcano-sedimentary rock (Charusiri et al., 1993). Evidence from whole-rock geochemistry indicated that this granite belt have characteristics of S-type granites (Charusiri et al., 1993; Schwartz et al., 1995; Wang et al., 2014). The extended Central Granite Belt in the north, Changning-Menglian Granite Belt, also has the same properties as the Central Granite Belt in Thailand (Wang et al., 2014). Evidence from $^{40}Ar/^{39}Ar$ technique shows the age of the Central Belt to 220 to 180 Ma or middle Late Triassic to late Early Jurassic (Charusiri, 1989). Afterwards, evidence from U-Pb zircon dating technique on Changning-Menglian Granite Belt defines the age ranging from 237 to 178 Ma or early Late Triassic to late Early Jurassic (BGMRY, Shi et al., 1989; 1990; Nie et al., 2012).

The Western Granite Belt extended from Southern China, Eastern Myanmar, Upper Southern and Western Thailand, and Western Sumatra (Charusiri et al., 1993; Wang et al., 2014). The country rocks where this granite intruded are Carboniferous to Permian clastic sedimentary rocks (Charusiri et al., 1993). Evidences from whole-rock geochemistry indicated that this granite belt have characteristics of S-type granites or ilmenite-series (Charusiri et al., 1993; Schwartz et al., 1995; Wang et al., 2015). The extended Western Granite Belt in the north, Tengchong-Baoshan Granite Belt, also has the same properties as the Western Granite Belt in Thailand (Wang et al., 2015). Initially, Rb-Sr dating for granites at Hermyingyi, Eastern Myanmar, which is located in the Western Granite Belt, defines age of 59±2 Ma with an initial $^{87}Sr/^{86}Sr$ ratio of 0.735±8 (Darbyshire and Swainbank, 1988). Later, $^{40}Ar/^{39}Ar$ dating technique was used to determine age of samples from Thailand and shows that these granite's age are ranging from 50 to 88 Ma or Late Cretaceous to Eocene (Charusiri et al., 1993). These granite can be classified into 2 units with ages ranging from 88 to 65 Ma and 60 to 50 Ma (Charusiri et al., 1993).

These granites are results of subduction and collision event in Southeast Asia (Charusiri et al., 1993; Sone and Metcalfe, 2008; Cobbing, 2011; Wang et al., 2014). On the one hand, the I-type Eastern Granite belt is believed to be an outcome from the subduction of Paleo-Tethys beneath Sibumasu Block during Late Permian to Early Triassic (Charusiri et al., 1993). On the other hand, the I-type Eastern Granite Belt is believed to derived from subduction of Paleo-Tethys beneath Indochina block during approximately Permian, forming Sukhothai Block (Sone and Metcalfe, 2008; Wang et al., 2014). Then, the S-type Central Granite Belt formed due to the collision between part of Sibumasu block (Shan-Thai block) and Sukhothai Terrane and Indochina block during Jurassic (Charusiri et al., 1993; Sone and Metcalfe, 2008; Wang et al., 2014). Finally, the S-type Western Granite Belt formed due to the collision between Western Myanmar block and Sibumasu block.

Tin-tungsten Deposits in Thailand

There are many standards to classify tin deposit types (eg. Varlamoff, 1975; Materikov, 1977; Taylor, 1979; Hosking, 1988). Hosking (1988) classified tin deposits into 13 major groups: (1) disseminations other than those in placers and that are not included in the other major groups; (2) pegmatites and/or aplites; (3) skarns; (4) hydrothermal breccias; (5) deposits associated with greisenized and/or albitized country rock; (6) stanniferous veins other than those of group 5; (7) godes of the Cornish type; (8) replacement (metasomatic) deposits that cannot be satisfactorily placed in any of the other groups; (9) telescoped, mineralogically complex deposits; (10) deposits of the Mexican type (epithermal or fumarole); (11) stanniferous massive sulfide and massive iron oxide deposits; (12) 'ancient', variously modified, stanniferous sedimentary deposits; and (13) 'modern' placers. These deposit types are illustrated in Figure 6 (Hosking, 1969)

In Thailand, we often found tin deposits associated with granite (Cobbing et al., 1986; Schwartz et al., 1995; Khin Zaw et al., 2014). According to the classification by Chappell and White (1974), tin deposits associated with granite are emplaced in S-type granite (Blevin and Chappell, 1995). Therefore, understanding in granite province in Thailand will lead to the location of tin deposits.
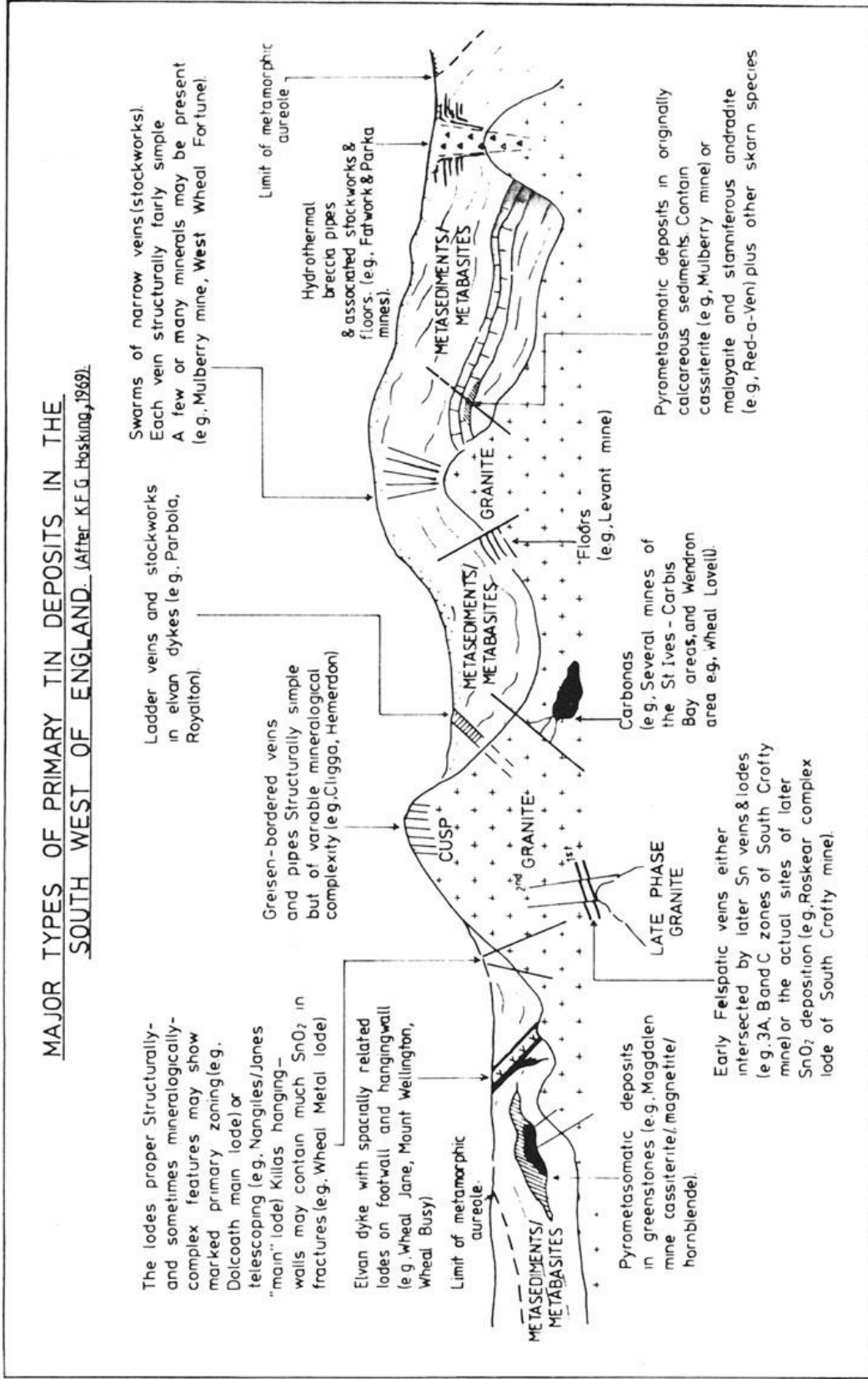
Figure 6 Major primary tin deposits types in the Southwest England (Hosking, 1969)

Background Geology of the Study Areas

Rock units in Study areas can be divided into three group: plutonic igneous rock unit, Permian Kaeng Krachan Group, and Ordovician Thung Song Group.

1. <u>Cretaceous – Eocene Granite</u>

Regarding the location of both study areas, petrography (Dheeradilok et al., 1985; Siribhakdi, Salyapongse, and Suteetorn, 1985; Kemlheg and Chiamton, 1989; Leewongcharoen and Chaturongkawanich, 1994), and geochemistry indicated that plutonic igneous rock in both areas are belonged to Cretaceous to Eocene, Western Granite Belt. Details were described in the previous topic.

2. <u>Permian Kaeng Krachan Group</u>

Chaodumrong, Assavapatchara, and Jongautchariyakul (2004) revised and merge Kaeng Krachan Group (Piyasin, 1973) and Phuket Group (Mitchell, Young, and Jautaranipa, 1970) into Kaeng Krachan Group of Early Permian. Kaeng Krachan Group is composed of 5 formations: Laem Mai Pai Formation, originally proposed by Hills (1989); Spillway Formation, originally proposed by Raksaskulwong and Wongwanich (1993); Ko He Formation, proposed by Raksaskulwong and Wongwanich (1993); Khao Phra Formation, proposed by Piyasin (1973); and Khao Chao Formation, proposed by Piyasin (1973) (Chaodumrong, 2010). Ko He Formation in Kaeng Krachan Group is also known as the Southeast Asian pebbly mudstone belt in north-south trend ranging from Lhasa, Western Yunnan, Myanmar, Western Thailand, Peninsular Thailand, and Peninsular Malaysia (Altermann, 1986; Chaodumrong, 2010; Ueno and Charoentitirat, 2011).

3. <u>Ordovician Thung Song Group</u>

Thung Song Group was first recognized as Thung Song Limestone (Brown et al., 1951). Then, Bunopas (1981) revised all Ordovician limestone which overlies Cambrian siliciclastic Tarutao Group conformably as Thung Song Group. Compare to Permian carbonates Ratburi Group, Thung Song Group is mostly a thin-bedded to massive, has micritic texture, and darker (Ridd, 2011). The Group consists of 7 formations (Wongwanich, 1990; Wongwanich et al., 2002). First, Malaka Formation, the bottommost formation which overlies Tarutao group conformably, is a very fine-bedded algal argillaceous limestone with burrows which deposited in intertidal environment (Wongwanich et al., 2002). Second, Talo Dang Formation is limestone interbedded with shale, deposited as lagoon (Wongwanich et al., 2002). Third, La Nga Formation is a cross-bedded algal limestone deposited as sand split (Wongwanich et al., 2002). Fourth, Pa Nan Formation is a stromatolitic limestone with burrows, nautiloids and sponges which deposited in subtidal environment (Wongwanich et al., 2002). Fifth, Lae Tong Formation is nodular limestone with occasional nautiloids and crinoids, deposited as lagoon (Wongwanich et al., 2002). Sixth, Rung Nok Formation is a biosparite, biolithite and limestone breccia with burrows, stromatoparoids, trilobites, nautiloids, crinoids and rare tabulate corals, deposited as shoaling and reef (Wongwanich, 1990). Finally, Pa Kae Formation, the uppermost formation of Ordovician Thung Song Group, is conformably superimposed by Silurian-Devonian-Carboniferous Thong Pha Phum Group (Wongwanich et al., 2002). Pa Kae Formation is a red stromatolitic limestone with red shale, deposited in a deep-water reef environment (Wongwanich, 1990; Wongwanich et al., 2002).

Introduction to Pilok and Takua Pit Thong Deposits

1.   <u>Pilok tin-tungsten deposit</u>

Pilok tin-tungsten deposit was classified as vein-type deposit (Mahawat, 1988). According to the classification by Hosking (1988), it is both group 5, deposits associated with greisenized and/or albitized country rock, and group 6, stanniferous veins other than those of group 5. The regional geology of Pilok area is dominated by the granites of Western Granite Belt and Devonian to Carboniferous folded clastic sequence of low-grade metamorphic rocks called Kaeng Krachan Formation (Lehmann et al., 1994) in Tanowsri Group, which is later revised and updated to Kaeng Krachan Group (Piyasin, 1973).

Granites in the area have several phases (Mahawat, 1988). The oldest phase of granites in this area is foliated K-feldspar megacrystic biotite-muscovite granite which can be subdivided into 3 sub-classes due to its texture: (1) K-feldspar megacrysts up to 40 mm large, on average 10-20mm; (2) medium- to coarse-grained porphyroclasts of K-feldspar, plagioclase (oligoclase) and quartz clusters; (3) fine-grained, blastomylonitic groundmass of quartz, alkali feldspar, biotite/chlorite, muscovite (Lehmann et al., 1994).

The mineralization in this area was found mainly in veins, veinlet, and stockworks (Lehmann et al., 1994). Cassiterite is confined in quartz veinlets and swarms of veinlets, whereas wolframite is found in quartz massive veins (Mahawat, 1988). In addition, most tin mineralization was found at the contact of aplite granite, whereas tungsten mineralization occurred in both granite and the country rock (Mahawat, 1988; Lehmann et al., 1994).

Granites in this area were dated by many works. Charusiri et al. (1993) suggested that granites are referred to Late Cretaceous (77 – 70 Ma), based on total fusion $^{40}Ar/^{39}Ar$ dating technique. SHRIMP U-Pb dating results of zircons grains in two monzogranite samples suggests the age in Toarcian period of early Jurassic (181.7±4.8 Ma and 175.3±3.3 Ma) (Shi et al., 2015)

2. <u>Takua Pit Thong tin-tungsten deposit</u>

Takua Pit Thong tin-tungsten deposit was classified as carbonate replacement sulfide cassiterite skarn (Suvansavate, 1986; Mahawat, 1988). According to the classification by Hosking (1988), it is classified as group 3: skarns (pyrometasomatic deposits). The regional geology of Takua Pit Thong area is dominated by the Western Granite Belt, Ordovician Thung Song Group, and Permian Kaeng Krachan Group (Suvansavate, 1986; Mahawat, 1988)

Granites in this area can be further classified into 2 groups: coarse-grained biotite-muscovite granite and fine- to medium-grained biotite (±muscovite, tourmaline) granite (Suvansavate, 1986). Pegmatitic and aplitic veins are also found with quartz veins in granites (Suvansavate, 1986). Charusiri (1989) suggested that granites are referred to Late Cretaceous (70 – 69 Ma), based on $^{40}Ar/^{39}Ar$ dating technique.

The cassiterite mineralization in this area was found at the contact of granite with calcareous country rock (Mahawat, 1988). The ore is composed of polymetallic oxides and sulfides (Suvansavate, 1986; Mahawat, 1988)

CHAPTER III
GRANITE CHARACTERISTIC

Field Observations and Petrography

From geological map, both Pilok and Takua Pit Thong deposits are associated with granite which intruded in Permian siliciclastic rock. Because of high degree of weathering and alteration due to tropical climate, and mineralization in the area, good condition outcrop of fresh rocks is extremely rare in both Pilok and Takua Pit Thong areas. Mostly, granitic rock outcrops were found as very high weathered exposures, which already turned into quartz-rich soil (Figure 9 to Figure 12). However, some good condition outcrop or very large loose block can be found in adjacent area.

In both area, two units of granitic rock can be distinguished from the field observation: porphyritic granite, and equigranular granite. In addition, there are another granitic rock which cannot be grouped to any facies because of its heavily weathering and alteration, called altered granitic rock. 11 and 9 samples of both porphyritic granite and equigranular granite were observed and collected from Pilok (Figure 7) and Takua Pit Thong (Figure 8), respectively, to represent the areas in further studies, i.e. petrography, geochemistry, and mineralogy.
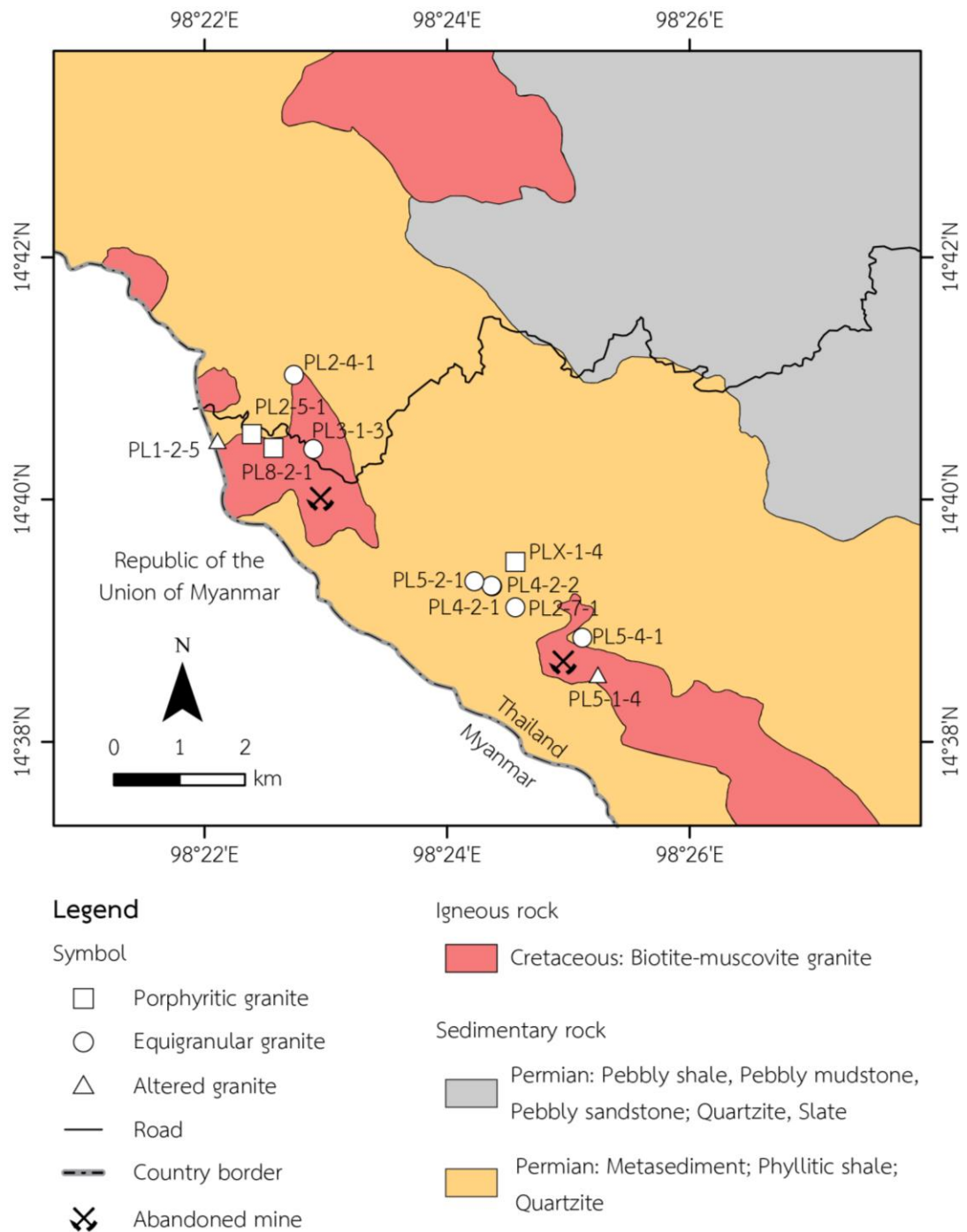
Figure 7 Geological map of Pilok area, Kanchanaburi Province (modified after Siribhakdi et al., 1985; Kemlheg and Chiamton, 1989; Chaodumrong, 2010) showing samples location
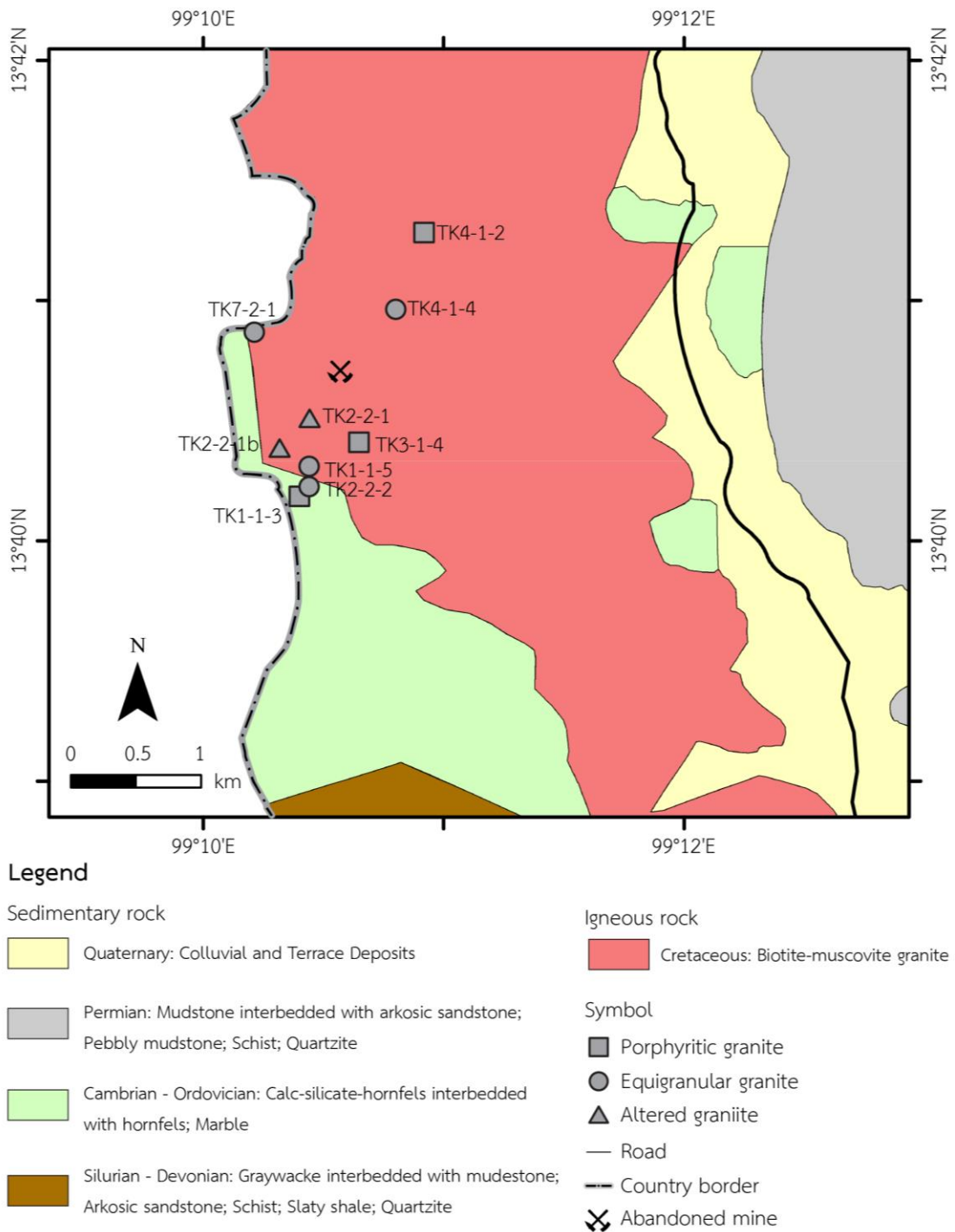
Figure 8   Geological map of Takua Pit Thong area, Ratchaburi Province (modified after Dheeradilok et al., 1985; Leewongcharoen and Chaturongkawanich, 1994; Chaodumrong, 2010) showing samples location
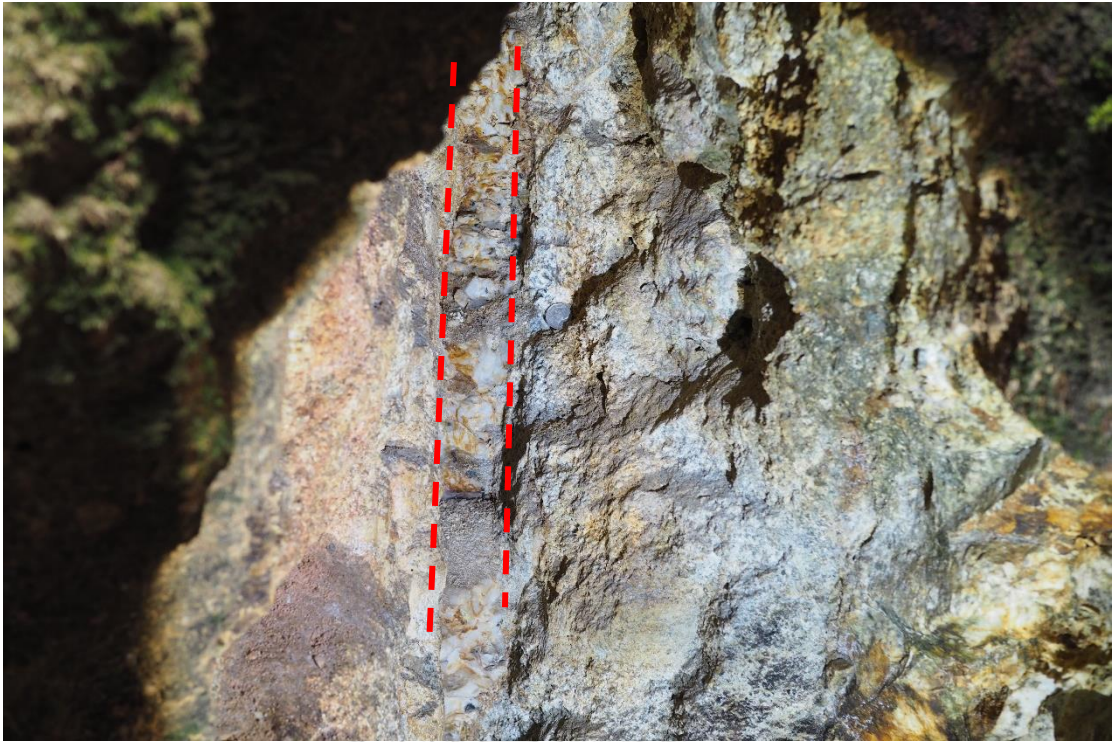
Figure 9 Outcrop of granitic rock in a tunnel at Pilok area containing 5 cm wide quartz vein and silicic alteration.

Figure 10 Altered granitic rock at Pilok area

Figure 11 Heavily altered and weathered granitic rock at Takua Pit Thong mine. Note that this is NOT a pile of soil because this can be seen all over the mining area
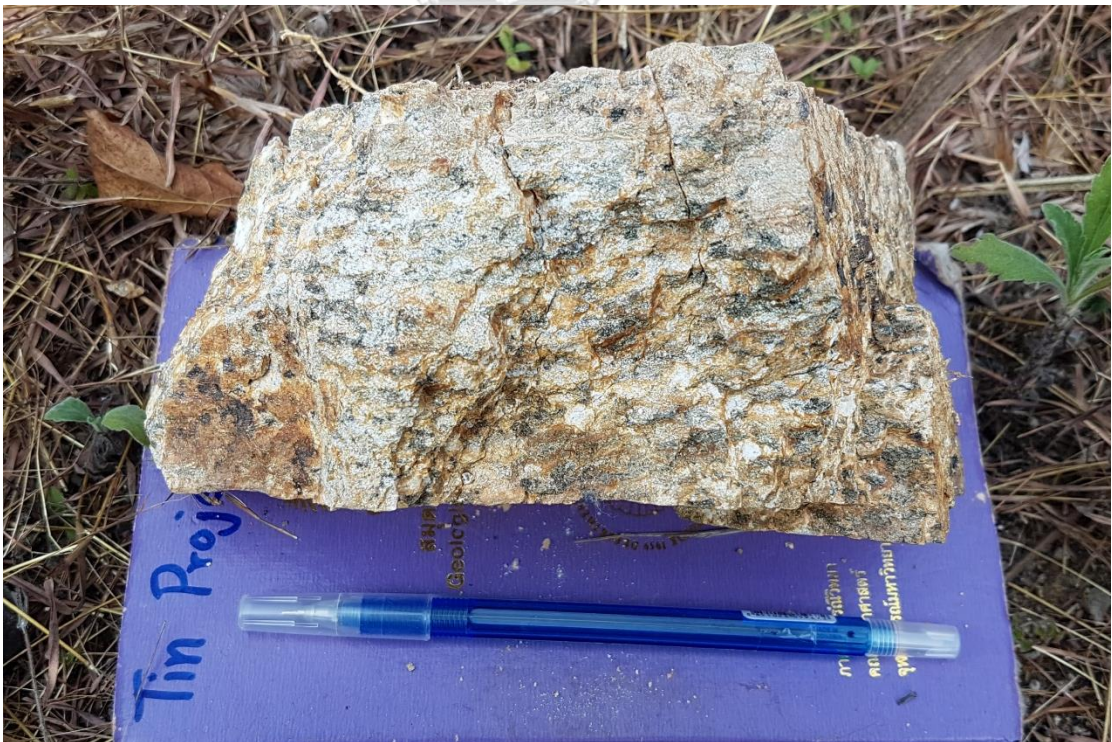
Figure 12 Altered granitic rock in Takua Pit Thong area

1. <u>Porphyritic granite</u>

Since granite outcrops in the mine were heavily weathered (Figure 9 and Figure 10), porphyritic granite cannot be found in the mining area but can be found outside the mine. Exposure of porphyritic granite is approximately 1 – 2 km away from the mines. The granitic rock found in these outcrops is plutonic igneous rock which has felsic composition. Its mineral assemblages are feldspar, quartz, plagioclase, biotite, and muscovite. So, they were classified in the field as granite. However, only some outcrops appeared biotite-muscovite granite (Figure 13). In usual, they appeared as biotite granite or chloritized biotite granite (Figure 14). As for the texture, they have phaneritic texture and porphyritic texture of feldspar, which is the characteristic feature to distinguish between porphyritic granite and other granitic rocks.

Using point-counting method, by dividing the thin sections into approximately 1,500 grids of 0.25 mm x 0.25 mm size, the petrographic study of porphyritic granite samples from Pilok (Figure 15a-d) and Takua Pit Thong (Figure 16a-b) shows mineral composition of 43 – 61 vol% orthoclase, 33 – 43 vol% quartz, 6 – 20 vol% plagioclase, 0 – 4 vol% biotite. According to QAP modal classification (Streckeisen, 1974), porphyritic granite are classified as alkali-feldspar granite to syenogranite (Figure 18). Accessories minerals are zircon, opaque minerals, and alteration product, i.e. sericite and chlorite (Figure 15b-d).

Degree of crystallinity of this granite is holocrystalline. Fine-grain quartz (0.1 – 0.5 mm) is found as anhedral crystals and shows weakly undulatory extinction. Also, it shows equigranular texture with fine-grained muscovite and biotite which are subhedral to euhedral grains (Figure 15a-d and Figure 16a, b). In contrary, medium-grained (2 – 5 mm) plagioclase (Figure 15b, d) and orthoclase (Figure 16b), are found as subhedral crystals and shows hiatal porphyritic texture with quartz, muscovite, and biotite. In addition, both orthoclase and plagioclase were altered to sericitized orthoclase and plagioclase (Figure 15b, d and Figure 16b). Moreover, orthoclase usually shows perthitic texture, the exsolution of Na-plagioclase from K-feldspar (Figure 16b).

Figure 13 Biotite granite showing porphyritic texture of feldspar at Hai Sok Waterfall, Pilok area

Figure 14 Chloritized biotite granite at Hai Sok Waterfall, Pilok area
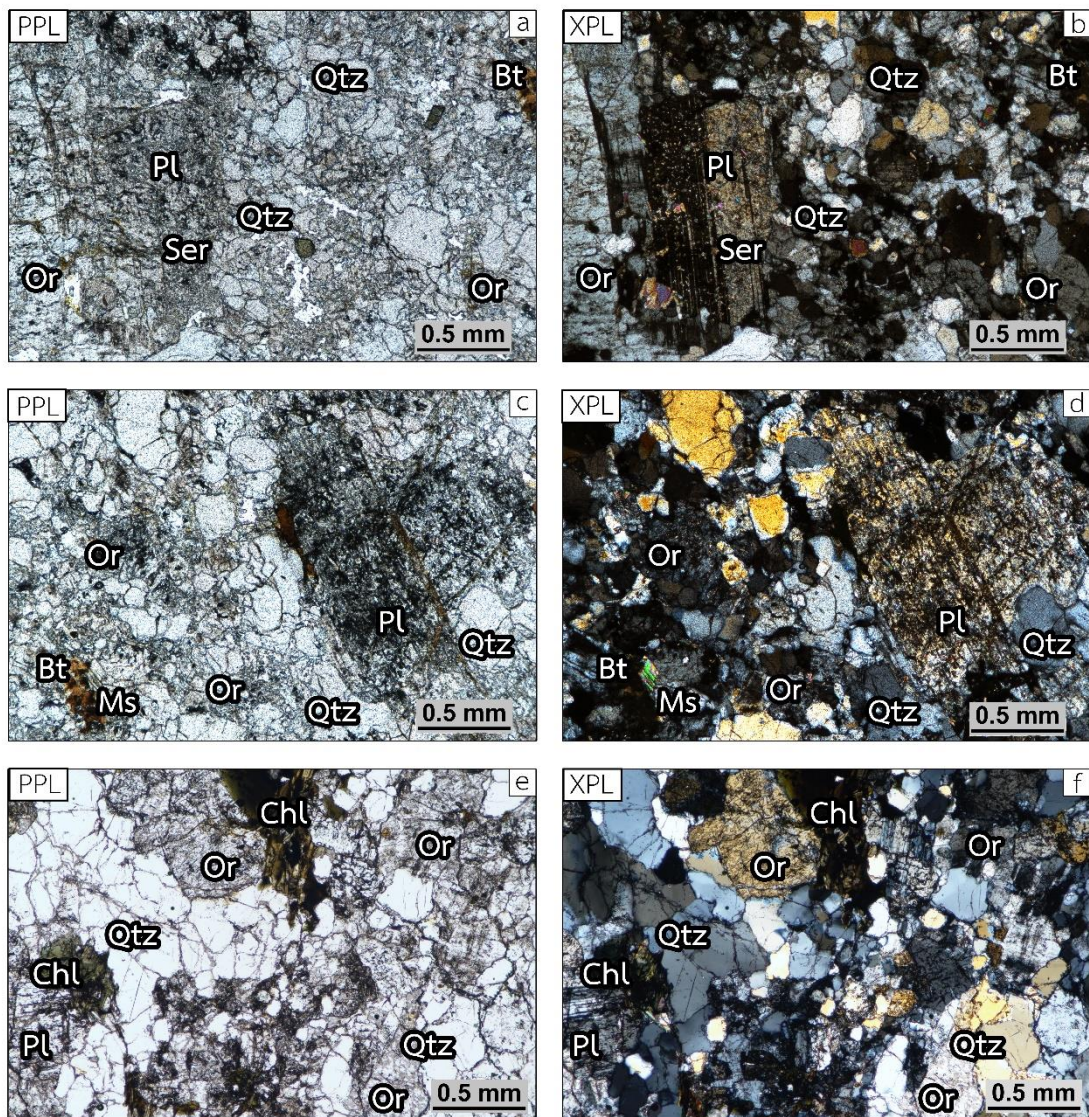
Figure 15 Photomicrograph under plane polarized light (PPL) and crossed polarized light (XPL) showing mineral assemblages and textures of granitic rocks from Pilok: (a) and (b) sample no. PL2-5-1, porphyritic granite under PPL and XPL, respectively; (c) and (d) sample no. PL8-2-1, porphyritic granite under PPL and XPL, respectively; (e) and (f) sample no. PL3-1-3, equigranular granite under PPL and XPL, respectively. Mineral abbreviations: Qtz = Quartz; Or = Orthoclase; Pl = Plagioclase; Ms = Muscovite; Bt = Biotite; Ser = Sericite; and Chl = Chlorite.
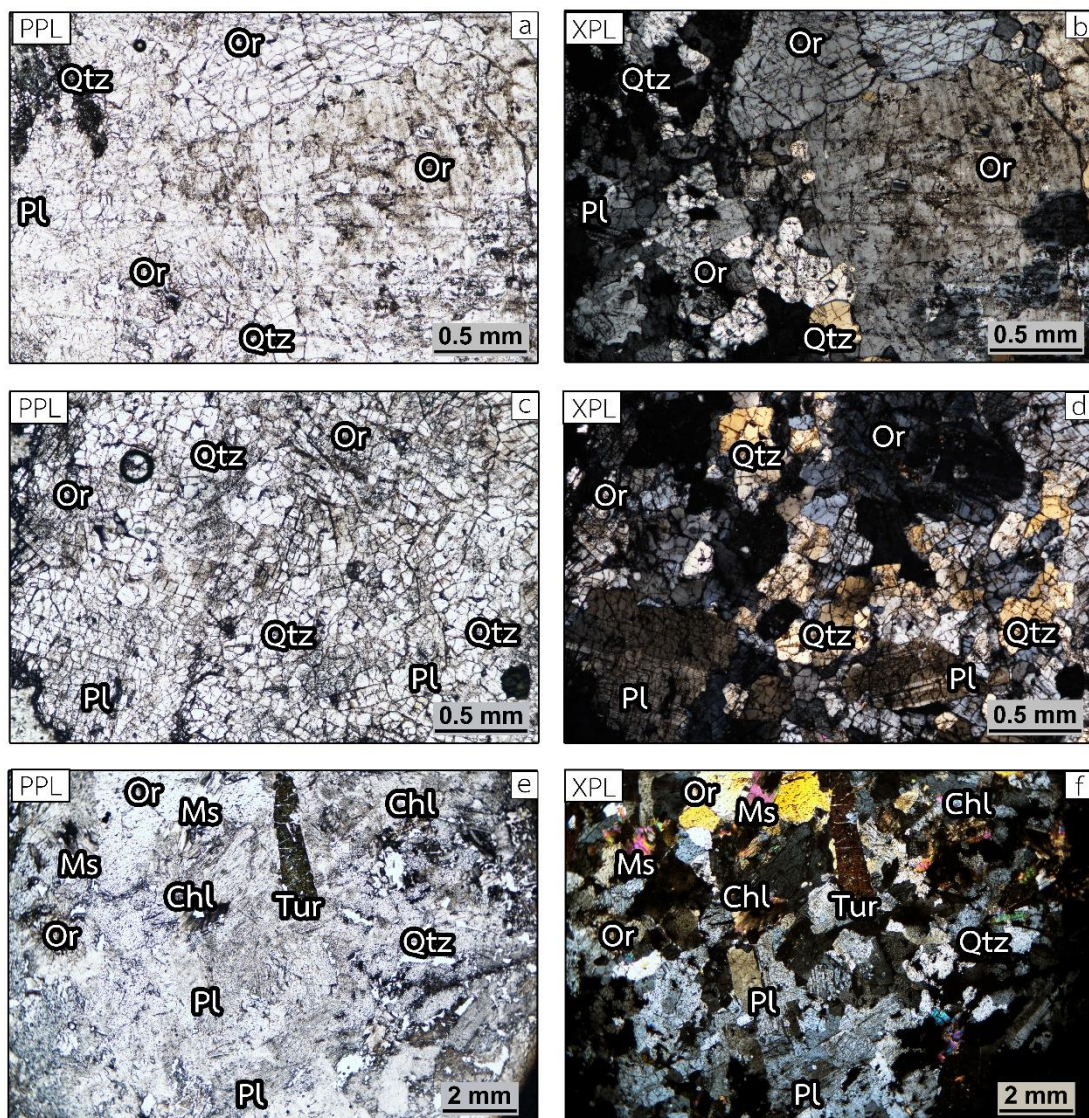
Figure 16 Photomicrograph under plane polarized light (PPL) and crossed polarized light (XPL) showing mineral assemblages and textures of granitic rocks from Takua Pit Thong: (a) and (b) sample no. TK3-1-4, porphyritic granite under PPL and XPL, respectively; (c) and (d) sample no. TK4-1-2, equigranular granite under PPL and XPL, respectively; (e) and (f) sample no. TK4-1-4, tourmaline granite (one of equigranular granite) under PPL and XPL, respectively. Mineral abbreviations: Qtz = Quartz; Or = Orthoclase; Pl = Plagioclase; Ms = Muscovite; Tur = Tourmaline; and Chl = Chlorite.
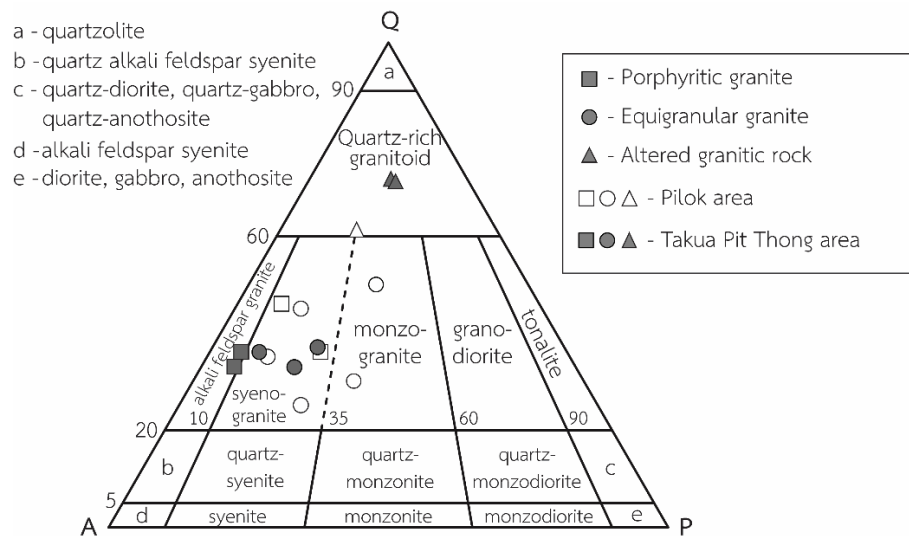
Figure 17 Modal QAP diagram (after Streckeisen, 1974) of thin sections from granitic rocks in Pilok and Takua Pit Thong area. Abbreviations are modal quartz (Q); modal alkali feldspar (A); and modal plagioclase (P).

2. Equigranular granite

Equigranular granite outcrops are exposed along the margin of both mines, covering an area of 1-2 sq. km. in each area. The granitic rock found in these outcrops are plutonic igneous rock which has felsic composition. Its mineral assemblages are feldspar, quartz, biotite, muscovite, and tourmaline. So, they are classified in the field as granite. This granite can be further classified according to the associated mafic mineral as feldspar granite (Figure 18), muscovite granite (Figure 19), and tourmaline-biotite-muscovite granite (Figure 20). As for the texture, they have phaneritic texture and equigranular texture, which is one of the characteristic features to distinguish equigranular granite from other granitic rock (Figure 20). The other characteristic feature is the presence of tourmaline as tourmaline granite and tourmaline-biotite-muscovite granite

Using the same point-counting method as in porphyritic granite thin sections, the petrographic study of equigranular granite from Pilok (Figure 15e-f, Figure 21a-d) and Takua Pit Thong (Figure 16c-f) reveal an assemblage of minerals: 25 – 44 vol% orthoclase, 23 – 53 vol% quartz, 9 – 29 vol% plagioclase, 0 – 11 vol% biotite, 0 – 8 vol% muscovite, 0 – 4 vol% tourmaline, and 0 – 3 vol% microcline. According to QAP modal classification (Streckeisen, 1974), equigranular granites are classified as syenogranite to monzogranite (Figure 17). Accessories minerals are zircon, opaque minerals, and alteration products, i.e. sericite and chlorite (Figure 15e-f and Figure 16e-f).

Despite the texture from macroscopic view is equigranular texture, the petrographic study says otherwise, and reveals its seriate porphyritic texture. This can be called microporphyritic texture (Figure 15f and Figure 16d). However, the same term, equigranular granite, is a more appropriated term since it can distinguish granites from the macroscopic view. Degree of crystallinity is holocrystalline. Fine- to medium-grain (0.5 - 2 mm) orthoclase and plagioclase appeared as subhedral grains showing seriate porphyritic texture with other minerals (Figure 15f and Figure 16d, f). Perthitic texture of orthoclase is also observed (Figure 15f and Figure 16f). Moreover, fine-grain quartz (0.25 – 0.5 mm) is found as anhedral crystals showing its weakly undulatory extinction and its equigranular texture with fine-grain muscovite and biotite. Medium-grain tourmaline (1 – 5 mm), if it appears, is found in some samples, as phenocryst showing its hiatal porphyritic texture with other minerals (Figure 16e-f and Figure 21c-d). In addition, orthoclase, microcline, and plagioclase also have sericitized texture, where they were partly altered to sericite.

Figure 18 Equigranular granite and sign of silicic alteration at the village water gate, Pilok area

Figure 19 Exposure of granitic rock on a nearby hill, 1 km northeast of Takua Pit Thong mine

Figure 20 Equigranular granite on the hill, Takua Pit Thong area
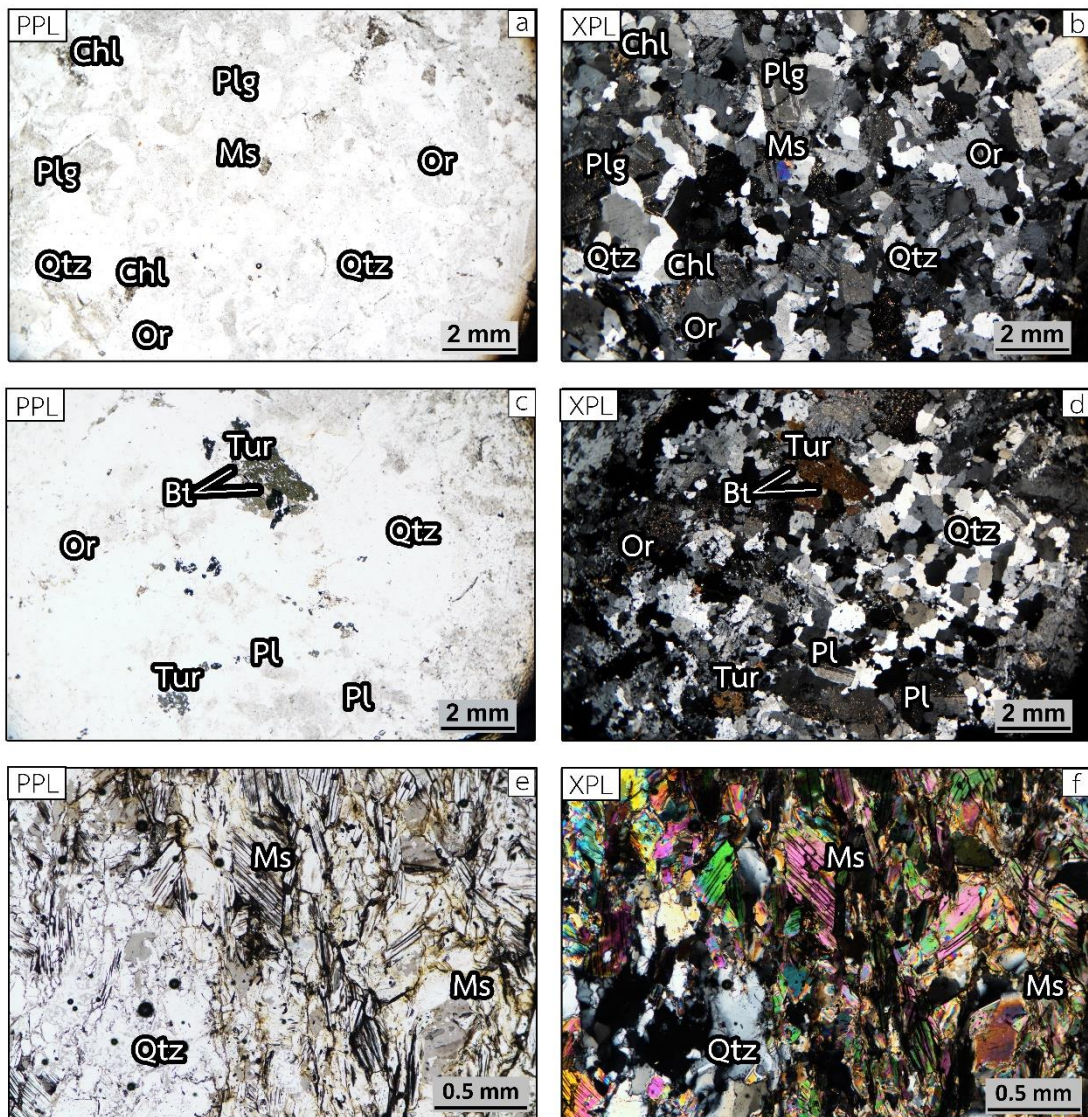
Figure 21 Photomicrograph under plane polarized light (PPL) and crossed polarized light (XPL) showing mineral assemblages and textures of granitic rocks from Pilok: (a) and (b) sample no. PL2-4-1, equigranular granite under PPL and XPL, respectively; (c) and (d) sample no. PL4-2-2, tourmaline granite (one of equigranular granite) under PPL and XPL, respectively; (e) and (f) sample no. 1-2-5, altered granitic rock under PPL and XPL, respectively. Mineral abbreviations: Qtz = Quartz; Or = Orthoclase; Pl = Plagioclase; Ms = Muscovite; Bt = Biotite; Tur = Tourmaline; and Chl = Chlorite

Whole-rock Geochemistry

Altered granitic rock samples are not analyzed for whole-rock geochemistry because of its heavily weathered condition. Major and minor oxides of granites from Pilok and Takua Pit Thong are shown in Table 1 and Table 2, respectively. Both granites showed similar Al_2O_3 and $Na_2O + K_2O$ composition, ranging from 12.72 to 20.86 wt.% and 6.01 to 9.08 wt.%, respectively. In addition, porphyritic granite revealed a higher value of total Fe and MgO, ranging from 0.03 to 2.87 w.t% and 0 to 0.25 wt.%, respectively, compared to those of equigranular granites which were ranging from 0.06 to 1.74 wt.%, 0 to 0.37 wt.%, respectively. In contrast, porphyritic granite had a lower value of SiO_2, CaO, and Na_2O, which are ranging from 59.07 to 69.46 wt.%, 0.03 to 0.67 wt.%, and 0.53 to 6.37 wt.%, respectively, than those of equigranular granite, which are ranging from 66.16 to 71.70 wt.%, 0.18 to 1.15 wt.%, 2.53 to 6.37 wt.%, respectively. However, XRF result of TiO_2 and MnO from both granites were widely distributed and cannot be compared. These major oxides and minor oxides are agreed with mineral assemblages from the petrographic studies, i.e. whole-rock geochemistry is a consequence of atoms in each mineral, such as high aluminum content from feldspar, and tourmaline.

Total alkali silica (TAS) chemical classification diagram (after Cox, Bell, and Pankhurst, 1979) was also used in addition to Streckeisen (1974) modal classification diagram. It showed relationship between silica content (SiO_2) and alkali content ($Na_2O + K_2O$). Even though the samples are not fresh, some key point can be made from this diagram. This discrimination diagram showed that porphyritic granite is quartz-diorite whereas equigranular granite is granite (Figure 22). Furthermore, all plots of porphyritic granite and equigranular granite show their subalkalne/tholeiitic composition (Figure 22) which is consistent with those plots in alkaline-FeO_{total}-MgO (AFM) ternary diagram (after Irvine and Baragar, 1971) showing calc-alkaline magmatic series (Figure 23). Harker variation plots (after Harker, 1909) of major and minor oxides against SiO_2 showed irregular, non-linear correlation, and constraint value of SiO_2 at the felsic composition (Figure 24a-h). Also, the two contrasting granite has different correlation trends for every major and minor oxides which represent their different magma suite.

Furthermore, a three-tier classification scheme for granitic rock (Frost et al., 2001), i.e. Fe* [FeO$_{total}$/(FeO$_{total}$ + MgO)], Modified Alkali-Lime Index (MALI), and Aluminium Saturation Index (ASI), was used to classify granites in this study. Plots between SiO$_2$ and Fe* mostly fall in ferroan rock region, leaving one of porphyritic granite from Pilok and four samples of equigranular granite from both areas in magnesian rock region (Figure 25a). However, these five contrasting samples fall very close to the boundary between ferroan rock and magnesian rock (Figure 25a). Also, Fe* was used as an alternative variable instead of Fe-number [FeO/(FeO+MgO)] because of the lack of ferric and ferrous iron value. As a result, both granites are classified as both ferroan rock and magnesian rock (Figure 25a), indicating a wide distribution on total iron. The secondary level of the classification plotted SiO$_2$ against Na$_2$O + K$_2$O − CaO, classified porphyritic granite as alkalic rock (Figure 25b), revealing abundance of alkali content and depletion of calcium. As for equigranular granite, it shows a wide distribution, ranging from alkalic rock to alkali-calcic rock (Figure 25b), which also suggest that alkali content is more abundant that calcium. The tertiary level of the classification plotted molecular ASI against Al/(Na + K), the molecular ratio Al/(Ca − 1.67P + Na +K). All plots fell in peraluminous rock region (Figure 25c), suggest an aluminium oversaturated magma series.

In summary, most of both granites revealed relatively low sodium, oversaturated in aluminium (molecular Al$_2$O$_3$/(Na$_2$O+K$_2$O+CaO) >1.1) (Figure 25c), restricted range of silica to felsic composition, and irregular interelement variation showing a non-linear correlation. These revelations leaded to a conclusion that both granites are S-type granite.

Table 1 Whole-rock geochemical analyses of major and minor oxides (wt.%) by XRF of granites from Pilok.

Rock type	Porphyritic granite			Equigranular granite						
Sample no.	PL2-5-1	PL8-2-1	PLX-1-4	PL2-4-1	PL2-7-1	PL3-1-3	PL4-2-1	PL4-2-2	PL5-1-3	PL5-1-5
SiO_2	63.41	66.50	62.80	68.32	71.07	72.27	69.74	71.35	70.75	69.10
Al2O3	14.77	19.01	20.75	14.42	15.29	13.93	15.01	14.31	17.85	18.12
FeO_{Total}	0.03	2.33	2.87	1.74	0.45	0.54	0.57	1.30	0.50	0.06
CaO	0.12	0.38	0.03	0.39	0.38	0.21	1.15	0.30	0.53	0.91
MgO	0.00	0.68	0.24	0.13	0.12	0.13	0.03	0.18	0.00	0.00
Na_2O	3.45	2.78	0.53	3.40	3.51	4.06	4.20	3.74	5.01	6.37
K_2O	4.11	5.14	6.55	4.64	5.17	4.26	4.64	4.74	4.00	2.71
P_2O_5	0.03	0.08	0.01	0.01	0.01	0.01	0.01	0.02	0.16	0.09
TiO_2	0.02	0.29	0.07	0.11	0.06	0.04	0.02	0.09	0.00	0.00
MnO	0.00	0.07	0.13	0.07	0.02	0.02	0.04	0.04	0.07	0.00
LOI	12.36	3.25	5.66	6.34	3.98	4.60	4.33	4.28	1.97	3.02
TOTAL	98.30	100.50	99.65	99.56	100.05	100.07	99.72	100.35	100.84	100.39

Table 2 Whole-rock geochemical analyses of major and minor oxides (wt.%) by XRF of granites from Takua Pit Thong.

Rock type	Porphyritic granite		Equigranular granite			
Sample no.	TK3-1-4	TK4-1-2	TK2-2-1c	TK2-2-2	TK4-1-4	TK7-2-1
SiO_2	66.00	63.47	69.74	70.74	70.12	68.88
$Al2O3$	17.74	17.57	13.98	15.45	16.04	17.81
FeO_{Total}	1.40	1.21	1.24	0.65	0.50	1.52
CaO	0.26	0.42	0.18	0.22	0.67	0.61
MgO	0.25	0.25	0.00	0.17	0.09	0.37
Na_2O	2.67	2.95	3.75	2.53	4.00	3.19
K_2O	4.25	4.35	2.26	5.12	3.86	5.22
P_2O_5	0.04	0.08	0.04	0.06	0.11	0.22
TiO_2	0.06	0.08	0.03	0.04	0.06	0.16
MnO	0.12	0.12	0.08	0.17	0.06	0.03
LOI	5.79	8.11	7.98	5.09	3.76	1.09
TOTAL	98.59	98.61	99.29	100.24	99.26	99.10
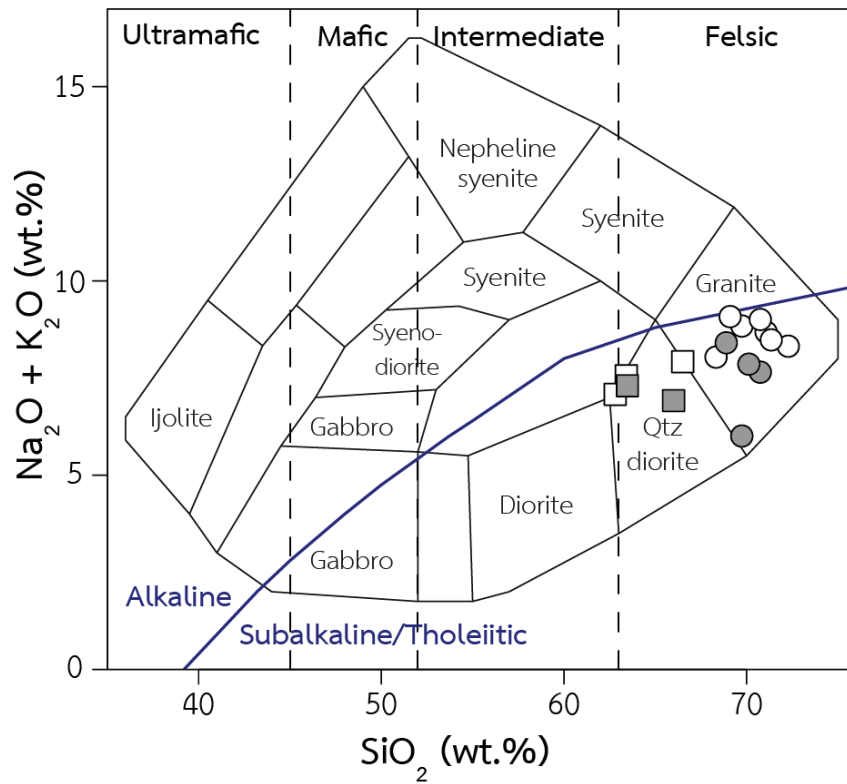
Figure 22   TAS diagram (after Cox et al., 1979) of granites from Pilok and Takua Pit Thong, plotting SiO₂ against Na₂O + K₂O. Rock symbols are as same as in Figure 23.
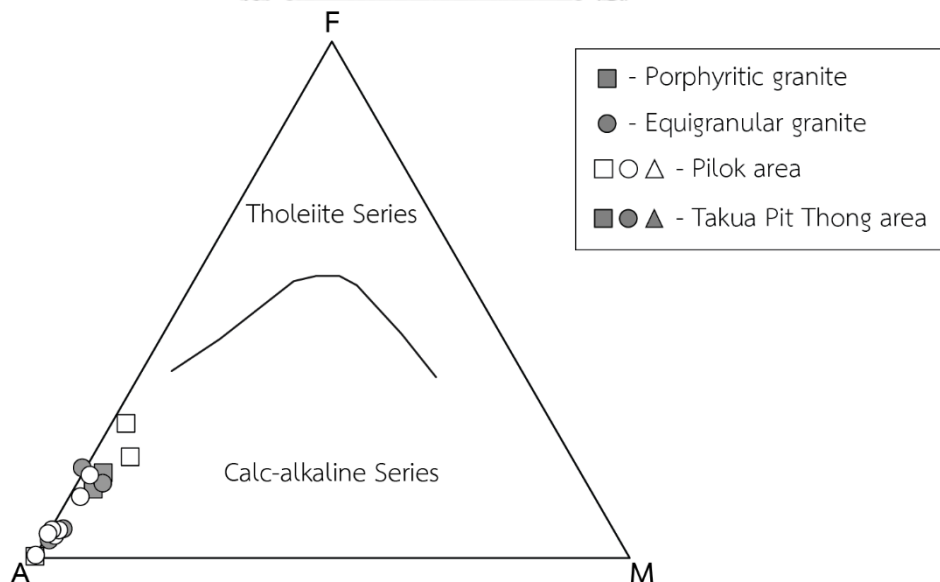
Figure 23 AFM diagram (after Irvine and Baragar, 1971) showing the calc-alkaline series of both porphyritic granite and equigranular granite from Pilok and Takua Pit Thong.
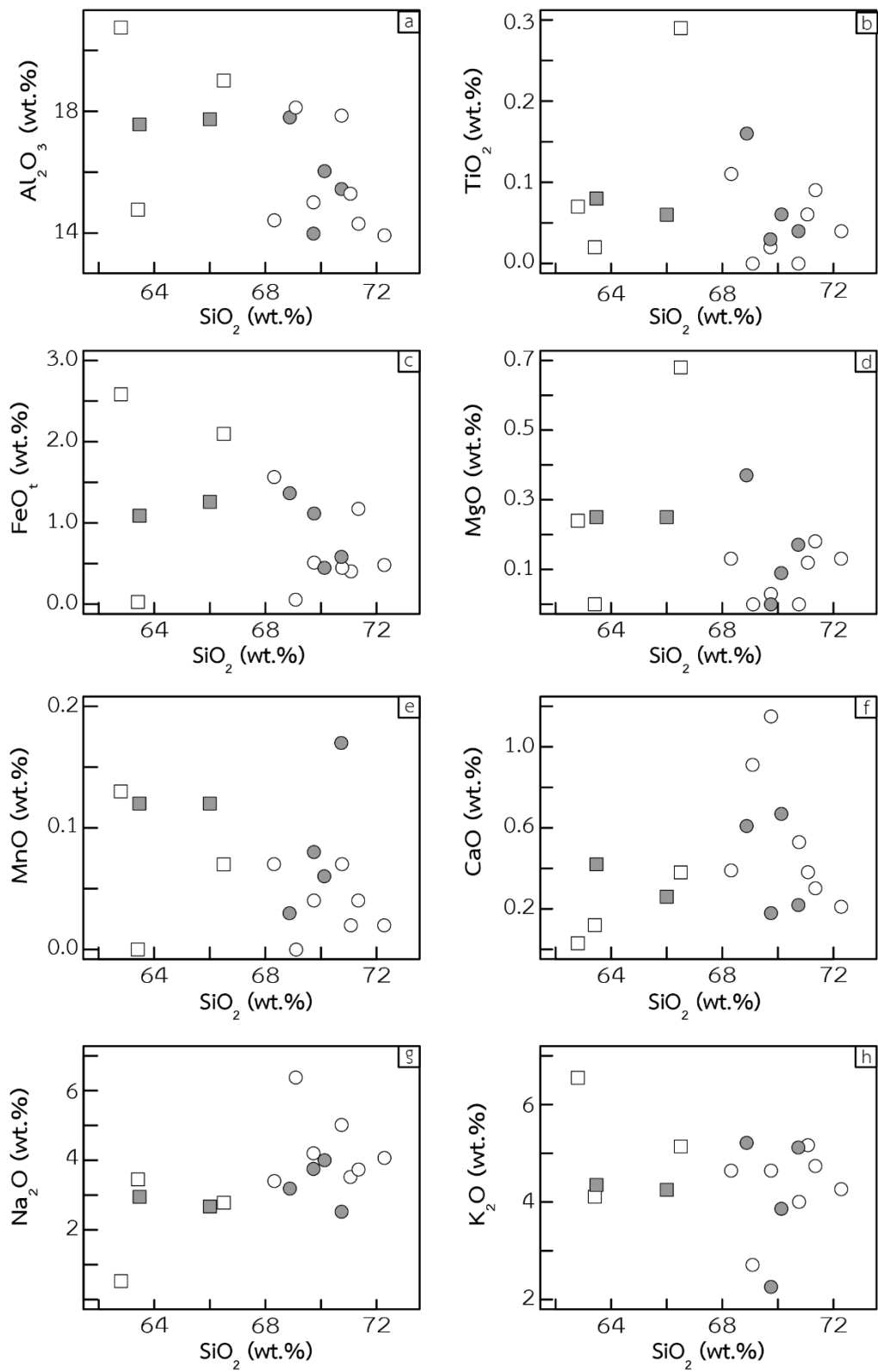
Figure 24 Harker variation diagram (after Harker, 1909), between SiO₂ and major oxides Rock symbols: white symbols = Pilok, grey symbols = Takua Pit Thong, square = porphyritic granite, circle = equigranular granite.
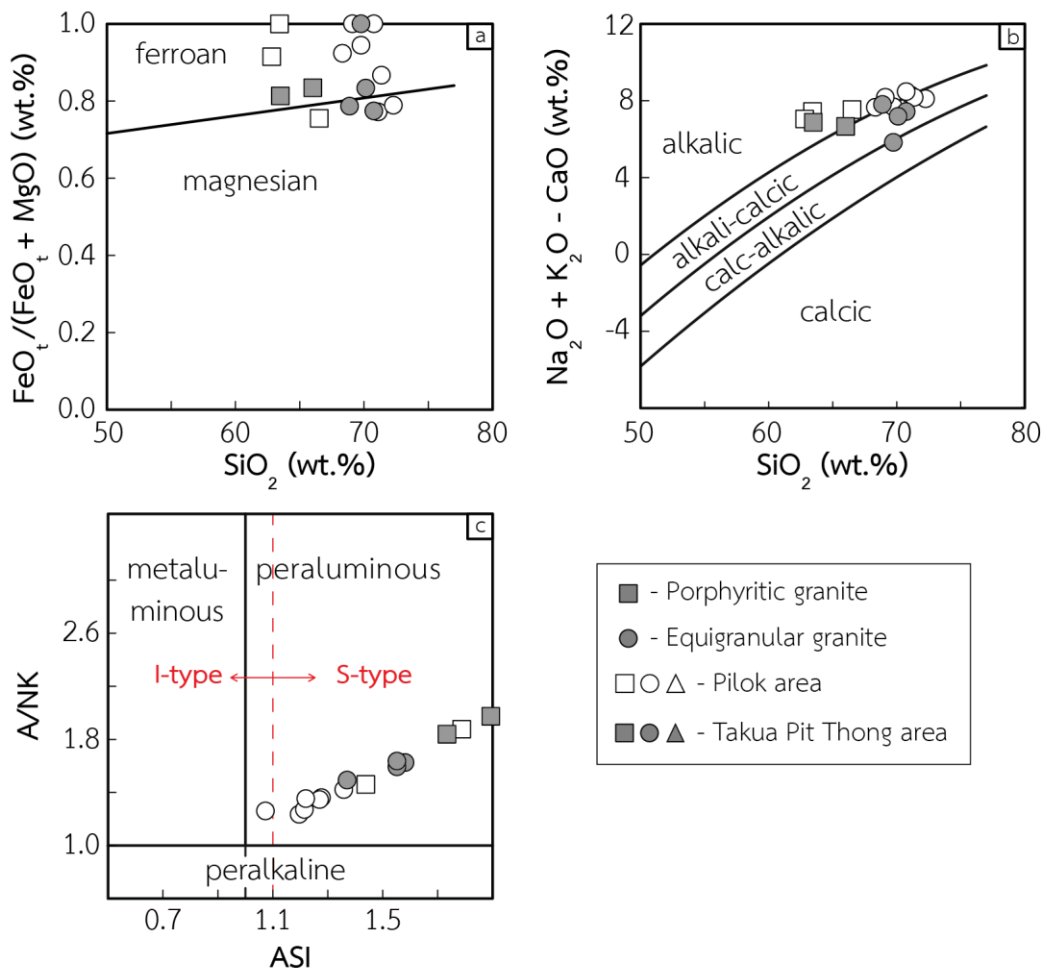
Figure 25 Granitic rock discrimination diagrams (modified after Frost et al., 2001) showing three-tiered classification scheme: (a) SiO$_2$ vs. Fe; (b) SiO$_2$ vs. MALI; and (c) ASI vs. A/NK.*

REE and Trace Elements

Trace elements and rare earth elements of granites from both areas are shown in Table 3. The primitive mantle-normalized (Sun and McDonough, 1989) spider diagram of porphyritic granite and equigranular granite from both Pilok and Takua Pit Thong (Figure 26a, c) show enrichment of U, Th, and Pb, inferring the presence of radioactive element in zircon and biotite. Furthermore, there are enrichment of some large ion lithophile elements (LILE), i.e. Cs, Rb, and K, and some of high field strength elements (HFSE). The normalized (Boynton, 1984) REE patterns (Figure 26b and Figure 26d) of the two granites show higher light-REE (LREE) than heavy-REE (HREE)

Table 3 *Whole-rock geochemical analyses of trace elements and REE (ppm) by ICP-MS of granites from Pilok and Takua Pit Thong*

Location	Pilok				Takua Pit Thong			
Rock type	Porphyritic granite		Equigranular granite		Porphyritic granite		Equigranular granite	
Sample no.	PL2-5-1	PL8-2-1	PL3-1-3	PL4-2-2	TK3-1-4	TK4-1-2	TK4-1-4	TK7-2-1
Ba	45.8	246	18.8	91.2	49.9	94.5	26.2	95.8
Ce	125	84.6	14.1	32.6	14.1	13.7	19	57.5
Cr	70	80	90	90	250	130	20	150
Cs	66.4	11.25	22.9	86.2	49.6	35.1	37.6	63.1
Dy	21.3	7.96	11.8	15.8	1.92	1.4	1.97	3.78
Er	14.8	5.18	7.96	11.6	1.3	0.81	1.16	1.87
Eu	1.25	0.51	0.05	0.25	0.14	0.14	0.13	0.23
Ga	17.5	17.8	18.6	18.2	43.2	35.5	31.2	29.2
Gd	17.35	6.99	6.79	9.44	1.6	1.33	1.49	4.05
Hf	4.8	6.2	2.5	2.8	3	1.3	1.5	3.5
Ho	4.71	1.64	2.47	3.64	0.39	0.27	0.37	0.69
La	66.9	43.8	7.3	16.7	6.7	6.3	8.9	25.6
Lu	2.74	1.03	1.31	1.88	0.24	0.15	0.23	0.27
Nb	37.9	28.7	38.9	59.3	109	73.4	73.5	42.6

Table 3 (continued) Whole-rock geochemical analyses of trace elements and REE (ppm) by ICP-MS of granites from Pilok and Takua Pit Thong

Location	Pilok				Takua Pit Thong			
Rock type	Porphyritic granite		Equigranular granite		Porphyritic granite		Equigranular granite	
Sample no.	PL2-5-1	PL8-2-1	PL3-1-3	PL4-2-2	TK3-1-4	TK4-1-2	TK4-1-4	TK7-2-1
Nb	37.9	28.7	38.9	59.3	109	73.4	73.5	42.6
Nd	89.9	32.7	7.8	17.1	6.1	5.3	7	21.7
Pb	74	49	78	64	38	39	29	41
Pr	25	9.46	1.86	4.36	1.56	1.45	2.14	6.08
Rb	499	436	515	446	1070	801	612	646
Sm	21.2	6.93	3.98	6.01	1.57	1.26	1.72	4.83
Sn	5	17	5	6	243	159	58	54
Sr	21.3	59.1	14.6	24.8	14.4	24.8	14.5	27.7
Ta	14.1	6.7	11.2	7.9	33	19	29	10.2
Tb	3.38	1.25	1.65	2.18	0.32	0.23	0.34	0.7
Th	39.2	44.4	17.9	39.6	8.74	6.86	13.15	30.2
Tm	2.57	0.9	1.29	1.86	0.22	0.13	0.22	0.29
U	19	13.4	22.2	36.2	4.88	4.85	35.5	23

Table 3 (continued) Whole-rock geochemical analyses of trace elements and REE (ppm) by ICP-MS of granites from Pilok and Takua Pit Thong

Location	Pilok				Takua Pit Thong			
Rock type	Porphyritic granite		Equigranular granite		Porphyritic granite		Equigranular granite	
Sample no.	PL2-5-1	PL8-2-1	PL3-1-3	PL4-2-2	TK3-1-4	TK4-1-2	TK4-1-4	TK7-2-1
U	19	13.4	22.2	36.2	4.88	4.85	35.5	23
V	5	19	6	7	2.5	6	2.5	2.5
W	16	2	6	6	21	23	12	11
Y	143	53	76.1	109	13.2	9	14.2	23.3
Yb	18.3	6.64	8.87	12.45	1.57	0.92	1.54	1.82
Zr	77	176	35	59	57	36	30	93
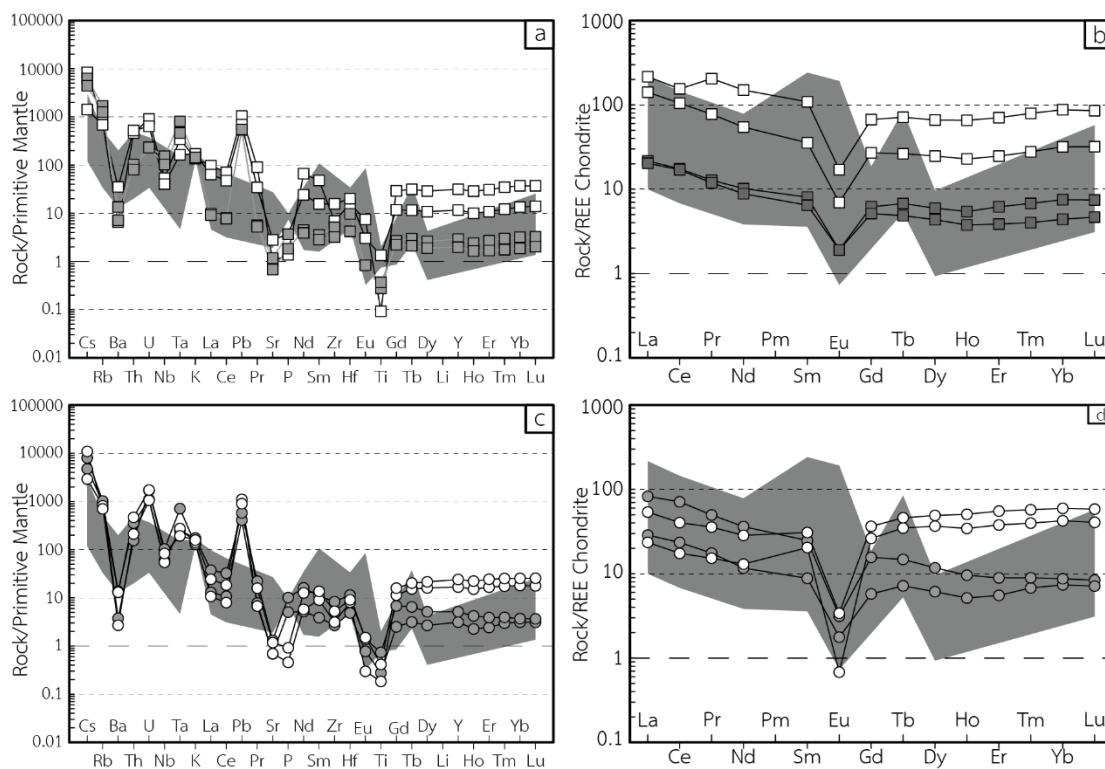
Figure 26   Normalized spider diagrams and REE pattern of granites from both areas in comparison with data from typical post-collision setting from Fourcade and Allegre (1981) presented as shade patterns: (a) and (c) primitive mantle-normalized spider diagrams (value from Sun and McDonough, 1989) of porphyritic granite and equigranular granite, respectively, from Pilok and Takua Pit Thong; (b) and (d) REE chondrite-normalized REE patterns (value from Boynton, 1984) of porphyritic granite and equigranular granite, respectively, from both areas. Rock type symbols: white symbols = Pilok, grey symbols = Takua Pit Thong, square = porphyritic granite, circle = equigranular granite.

CHAPTER IV

MINERALIZATION AND MINERAL CHEMISTRY

This chapter gathered information on ore and gangue mineral of ore zones from Pilok and Takua Pit Thong tin-tungsten deposits to determine the paragenesis of both areas. Moreover, mineral chemistry of feldspar and tourmaline were analyzed using EPMA to establish the mineral chemistry characteristics of both study areas.

Introduction

The focus of this study will be given to ore the petrographic study based on available polished mounts stored at Department of Geology, Faculty of Science, Chulalongkorn University. Additional surface samples collected during this fieldwork also will be used. However, suitable surface samples are rare due to strong oxidized. Previous studies were based on samples collected from mine areas that are not suitable after about 30 years mine shut down. The lack of samples (e.g. diamond drill cores and surface samples) making it is impossible to establish a paragenesis sequence during this study. Therefore, a paragenesis sequence will be mainly based on the previous established by Mahawat (1988), and Lehmann et al. (1994). In this study, details mineral paragenesis, mineral assemblages and textural features will be access and improved and confirmed by EPMA spot analysis and EPMA mapping. Petrographic study and analyses at from this study were accomplished using a reflected light microscope. Crystal morphology, mutual grain boundary relationship, crosscutting relationship, and mineral replacement were used to establish the paragenesis sequence of different mineralization stages (Craig and Vaughan, 1994).

Each minerals were identified using their optical properties (Craig and Vaughan, 1994) and confirmed by EPMA as shown in Table 4, Table 5, and Table 6.

Table 4 Mineral chemical analyses of quartz grains from Takua Pit Thong.

Sample No.	ORB-1-4-2-C1	ORB-1-21-C3		
Analysis No.	Qtz-2	Qtz-1	Qtz-2	Qtz-3
Oxides (wt%)				
SnO_2	0.004	0.003	0.000	0.021
FeO_{total}	0.314	0.031	0.003	0.000
WO_3	0.017	0.000	0.109	0.005
CaO	0.000	0.000	0.001	0.010
MnO	0.020	0.000	0.000	0.000
Al_2O_3	0.000	0.000	0.036	0.022
SiO_2	100.506	99.548	99.899	99.037
K_2O	0.007	0.000	0.007	0.008
Total	100.868	99.582	100.055	99.103

Table 5 Mineral chemical analyses of pyrrhotite grains from Takua Pit Thong.

Sample No.	ORB1-4-2-C1					ORB1-4-2-C2			ORB1-8-C1		ORB1-8-C5
Analysis No.	1	2	3	11	12	4	5	6	1	6	2
Elements (wt.%)											
As	0.00	0.00	0.04	0.00	0.00	0.00	0.00	0.01	0.00	0.00	0.00
Sn	0.00	0.00	0.00	0.00	0.00	0.00	0.00	0.00	0.00	0.00	0.00
Fe	65.83	65.23	64.14	64.38	65.16	64.75	64.52	64.34	62.63	62.74	62.83
W	0.00	0.05	0.00	0.00	0.00	0.00	0.03	0.00	0.00	0.00	0.00
S	34.14	33.13	35.62	34.27	34.69	34.13	34.96	34.27	37.79	37.99	36.99
Mo	0.37	0.43	0.44	0.42	0.41	0.42	0.42	0.35	0.36	0.36	0.35
Bi	0.00	0.00	0.00	0.00	0.00	0.00	0.00	0.00	0.00	0.00	0.00
Cu	0.00	0.00	0.00	0.09	0.03	0.04	0.11	0.32	0.00	0.00	0.00
Ca	0.00	0.00	0.00	0.00	0.00	0.00	0.00	0.00	0.00	0.00	0.00
Mn	0.00	0.01	0.02	0.02	0.00	0.04	0.04	0.00	0.00	0.03	0.00
Zn	0.00	0.00	0.01	0.03	0.01	0.03	0.01	0.02	0.01	0.05	0.03
Total	100.34	98.84	100.23	99.21	100.29	99.41	100.09	99.30	100.79	101.16	100.19

Table 5 *Mineral chemical analyses of pyrrhotite grains from Takua Pit Thong*

Sample No.	ORB1-4-2-C1					ORB1-4-2-C2			ORB1-8-C1		ORB1-8-C5
Analysis No.	1	2	3	11	12	4	5	6	1	6	2
Number of ions based on 1 S											
As	0.00	0.00	0.00	0.00	0.00	0.00	0.00	0.00	0.00	0.00	0.00
Sn	0.00	0.00	0.00	0.00	0.00	0.00	0.00	0.00	0.00	0.00	0.00
Fe	1.11	1.13	1.03	1.08	1.08	1.09	1.06	1.08	0.95	0.95	0.98
W	0.00	0.00	0.00	0.00	0.00	0.00	0.00	0.00	0.00	0.00	0.00
S	1.00	1.00	1.00	1.00	1.00	1.00	1.00	1.00	1.00	1.00	1.00
Mo	0.00	0.00	0.00	0.00	0.00	0.00	0.00	0.00	0.00	0.00	0.00
Bi	0.00	0.00	0.00	0.00	0.00	0.00	0.00	0.00	0.00	0.00	0.00
Cu	0.00	0.00	0.00	0.00	0.00	0.00	0.00	0.00	0.00	0.00	0.00
Ca	0.00	0.00	0.00	0.00	0.00	0.00	0.00	0.00	0.00	0.00	0.00
Mn	0.00	0.00	0.00	0.00	0.00	0.00	0.00	0.00	0.00	0.00	0.00
Zn	0.00	0.00	0.00	0.00	0.00	0.00	0.00	0.00	0.00	0.00	0.00

Table 6 Mineral chemical analyses of chalcopyrite grains from Takua Pit Thong.

Sample No.	ORB-1-4-2-C1			ORB-1-4-2-C2			ORB-1-8-C2		
Analysis No.	8	9	10	7	8	9	1	3	7
Elements (wt.%)									
As	0.00	0.00	0.04	0.00	0.00	0.02	0.00	0.00	0.00
Sn	0.00	0.00	0.00	0.00	0.00	0.00	0.00	0.00	0.00
Fe	31.72	32.27	31.69	31.19	32.41	32.20	32.49	32.25	33.53
W	0.00	0.00	0.00	0.00	0.00	0.01	0.03	0.00	0.00
S	29.13	29.26	29.35	29.77	27.61	27.27	29.30	28.63	28.68
Mo	0.44	0.36	0.42	0.43	0.33	0.42	0.37	0.39	0.39
Bi	0.00	0.00	0.00	0.00	0.00	0.00	0.00	0.00	0.00
Cu	37.76	37.79	38.15	37.66	39.18	39.76	37.71	38.64	38.15
Ca	0.00	0.00	0.00	0.00	0.00	0.00	0.00	0.00	0.00
Mn	0.00	0.00	0.00	0.04	0.06	0.00	0.01	0.00	0.02
Zn	0.03	0.00	0.01	0.00	0.01	0.05	0.00	0.03	0.00
Total	99.07	99.68	99.61	99.09	99.59	99.71	99.91	99.95	100.77

Table 6 Mineral chemical analyses of chalcopyrite grains from Takua Pit Thong.

Sample No.	ORB-1-4-2-C1			ORB-1-4-2-C2			ORB-1-8-C2		
Analysis No.	8	9	10	7	8	9	1	3	7
	Number of ions based on 2 S								
As	0.00	0.00	0.00	0.00	0.00	0.00	0.00	0.00	0.00
Sn	0.00	0.00	0.00	0.00	0.00	0.00	0.00	0.00	0.00
Fe	1.25	1.27	1.24	1.20	1.35	1.36	1.27	1.29	1.34
W	0.00	0.00	0.00	0.00	0.00	0.00	0.00	0.00	0.00
S	2.00	2.00	2.00	2.00	2.00	2.00	2.00	2.00	2.00
Mo	0.01	0.01	0.01	0.01	0.01	0.01	0.01	0.01	0.01
Bi	0.00	0.00	0.00	0.00	0.00	0.00	0.00	0.00	0.00
Cu	1.31	1.30	1.31	1.28	1.43	1.47	1.30	1.36	1.34
Ca	0.00	0.00	0.00	0.00	0.00	0.00	0.00	0.00	0.00
Mn	0.00	0.00	0.00	0.00	0.00	0.00	0.00	0.00	0.00
Zn	0.00	0.00	0.00	0.00	0.00	0.00	0.00	0.00	0.00

Mineralization

These stages can be divided into three stages: the tin-tungsten ore stage; the main sulfides stage, and the post-Sn-W mineralization stage.

1. Stage 1: the tin-tungsten ore stage

Both Pilok and Takua Pit Thong deposits show similar mineral assemblages with minor different in this stage. At Pilok, stage 1 mineralization is characterized by quartz-biotite-feldspar-cassiterite-wolframite-chalcopyrite assemblage (Figure 27), whereas Takua Pit Thong is characterized by quartz-biotite-feldspar-cassiterite-wolframite-arsenopyrite assemblage (Figure 28). Based on the textural relationships suggesting quartz, biotite and feldspar formed earlier than cassiterite and wolframite (Figure 29 and Figure 30). At Pilok, small amount of chalcopyrite is closely associated with cassiterite (Figure 29). However, there is enough evidence that the forming of cassiterite and/or wolframite was followed by the forming of arsenopyrite and the sulfide mineral forming stage. In addition, cassiterite and wolframite from Pilok occurs in quartz vein (Figure 31 and Figure 32), whereas cassiterite and wolframite from Takua Pit Thong occurs in skarns.

2. Stage 2: the main sulfides stage

There is a slightly different paragenetic sequence of the sulfide mineral forming stage between the two deposits. At Pilok, the mineral assemblages are quartz-biotite-feldspar-chalcopyrite-pyrite-sphalerite (Figure 27). In contrast, at Takua Pit Thong, the mineral assemblages are quartz-biotite-feldspar-pyrrhotite-pyrite-chalcopyrite-sphalerite-arsenopyrite (Figure 28). Particularly, the difference is presence and relationship of pyrrhotite and arsenopyrite at Takua Pit Thong along with chalcopyrite, pyrite, and sphalerite (Figure 30). Based on the textural relationships suggesting quartz, biotite and feldspar formed earlier than the main sulfide minerals (Figure 29 and Figure 30).

3. Stage 3: the post tin-tungsten mineralization stage

This mineralization stage refers to any mineralization which occurred after the main mineralization phase. Both deposits have the same paragenetic sequence: chlorite-quartz and other alteration product (Figure 27 and Figure 28). The difference of quartz between the one in the pre-mineralization stage and in this stage is the size, shape, and the mineral association. Quartz in this paragenetic sequence is smaller and more anhedral than quartz in the pre-mineralization stage. As for chlorite, it replaced biotite in the pre-mineralization stage.

จุฬาลงกรณ์มหาวิทยาลัย
CHULALONGKORN UNIVERSITY

Mineral \ Stage		Stage 1: Tin-tungsten	Stage 2: Main Sulfides	Stage 3: Post-mineralization
Ore	Cassiterite	————		
	Wolframite	———		
	Pyrite		————	
	Chalcopyrite		————	
	Sphalerite		————	
Gangue	Quartz	———	———	————
	Biotite	———	———	
	Feldspar	———	———	
	Chlorite			————

Figure 27 Paragenetic diagram showing the occurrence and relative abundance of ore and gangue minerals of Pilok tin-tungsten deposit

Mineral \ Stage		Stage 1: Tin-tungsten	Stage 2: Main Sulfides	Stage 3: Post-mineralization
Ore	Cassiterite	————		
	Wolframite	———		
	Pyrite		————	
	Chalcopyrite		————	
	Sphalerite		————	
	Arsenopyrite	————		
	Pyrrhotite		————	
Gangue	Quartz	———	———	————
	Biotite	———	———	
	Feldspar	———	———	
	Chlorite			————

Figure 28 Paragenetic diagram showing the occurrence and relative abundance of ore and gangue minerals of Takua Pit Thong tin-tungsten deposit
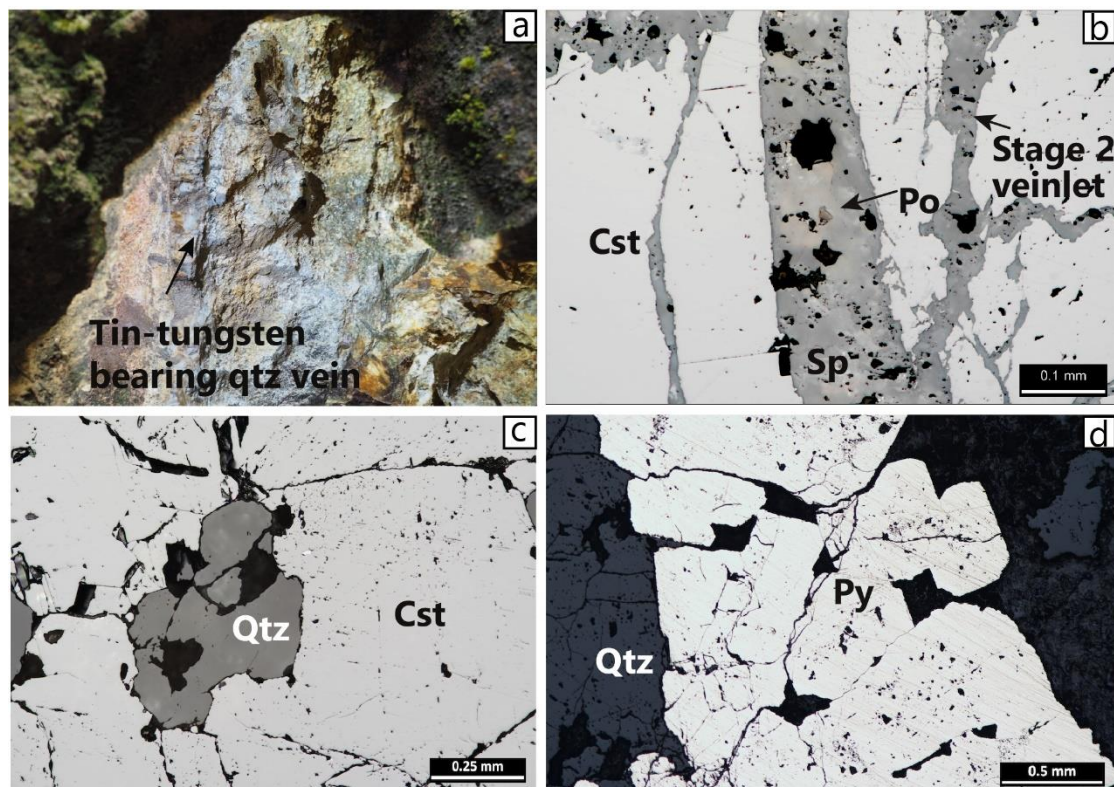
Figure 29 Photomicrograph of ore and gangue mineral in quartz veins from Pilok: (a) Exposure of tin-tungsten bearing quartz vein associated with altered granitic rock; (b) Cross-cutting relationship of stage 2 veinlet into stage 1 minerals; (c) Relationship between quartz; (d) Relationship between quartz of early stage 2 and pyrite of late stage 2. Mineral abbreviations are Qtz = Quartz; Cst = Cassiterite; Sp = Sphalerite; and Py = Pyrite.
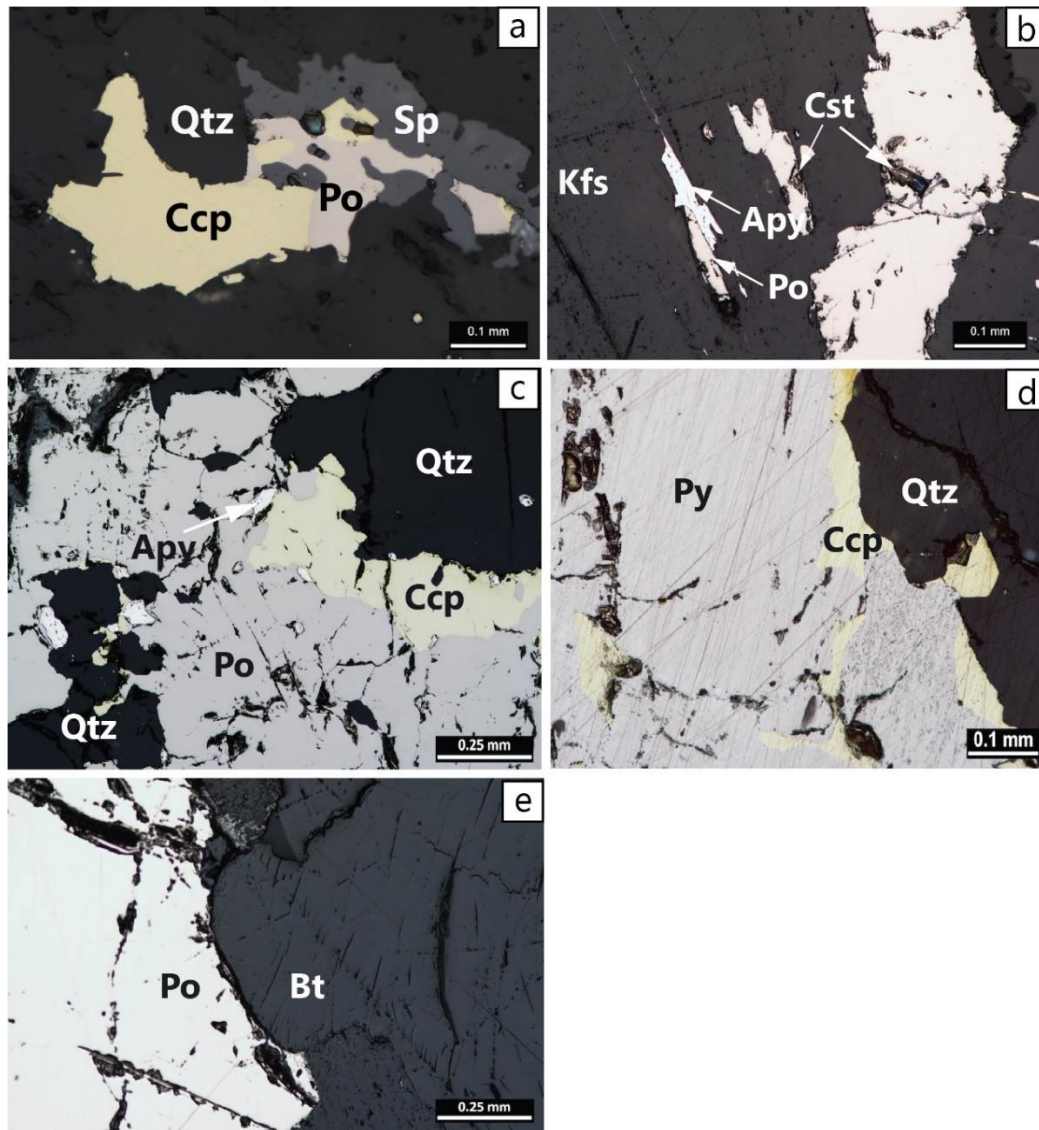
Figure 30 Photomicrograph of ore and gangue mineral associated with granite and skarn from Takua Pit Thong using a reflected light microscope: (a) Sample OTK3-showing anhedral quartz of early stage 2 and fine- to medium grain chalcopyrite, pyrrhotite, and sphalerite of late stage 2;; (b) Sample ORB1-15 showing K-feldspar of early stage 1 and fine-grained cassiterite, arsenopyrite, and pyrrhotite of late stage 1; (c) Sample ORB1-11-2 showing fine-grained anhedral quartz of early stage 2 associated with fine-grained arsenopyrite, chalcopyrite, and pyrrhotite of late stage 2; (d) Sample OTK1-1 showing subhedral quartz of early stage 2 associated with medium-grained pyrite and very fine-grained chalcopyrite of late stage 2; (e) Sample ORB1-8 showing fine- to medium-grained biotite of early stage 1 associated with fine- to medium-grained pyrrhotite of late stage 1. Mineral abbreviations are: Qtz = Quartz; Bt = Biotite; Ksf = K-feldspar; Cst = Cassiterite; Apy = Arsenopyrite; Sp = Sphalerite; Py = Pyrite, Ccp = chalcopyrite; and Po = Pyrrhotite.

Figure 31 Wolframite-arsenopyrite bearing quartz vein in granitic rock from Pilok area

Figure 32 Cassiterite bearing quartz vein in granitic rock from Pilok area

Mineral Chemistry

Mineral chemistry compositions of solid-solution minerals, i.e. K-feldspar, plagioclase, and tourmaline, in porphyritic granite and equigranular granite were analyzed using an electron microprobe.

1. <u>Feldspar</u>

K-feldspar and plagioclase in porphyritic granite and equigranular granite from Pilok and Takua Pit Thong were analyzed and presented in Table 7, Table 8, and Table 9. K-feldspar from all granites shows similar composition, ranging from 94%Or to 96%Or, which fall in orthoclase field (Figure 33a-b).. Plagioclase from all granites also show similar value, fall within Albite field. An content is ranging from 1%An to 5%An (Figure 33a-b).
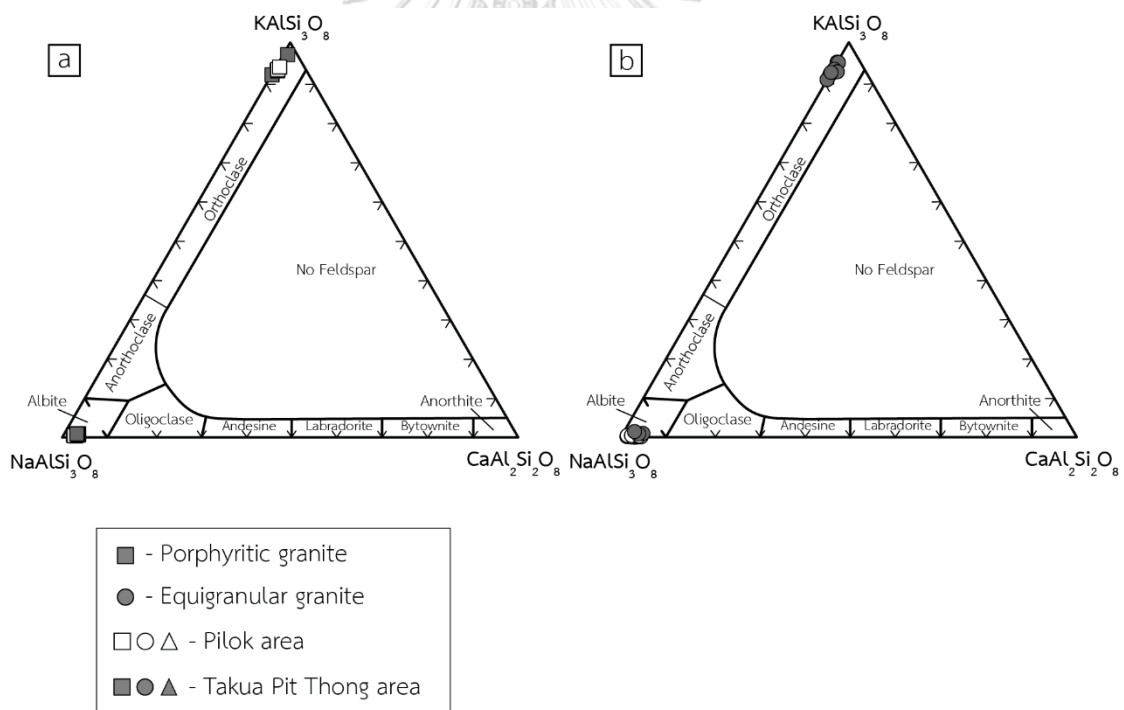
Figure 33 Plots of mineral chemistry of feldspar in granitic rocks from Pilok and Takua Pit Thong area: (a) porphyritic granite; and (b) equigranular granite.

Table 7 *Mineral chemical analyses of feldspar grains in porphyritic granite from Pilok area*

Sample	PL2-5-1								PL8-2-1			
SiO$_2$	69.28	69.04	68.71	68.87	69.62	65.95	65.91	65.71	69.28	68.95	69.81	67.28
Al$_2$O$_3$	16.93	17.30	17.64	18.00	17.84	16.21	15.93	16.28	18.20	18.19	17.86	19.37
FeO$_{Total}$	0.04	0.00	0.00	0.07	0.05	0.03	0.01	0.02	0.00	0.04	0.01	0.00
MgO	0.00	0.00	0.00	0.00	0.01	0.00	0.01	0.02	0.00	0.00	0.00	0.00
CaO	0.42	0.53	0.54	0.97	0.48	0.00	0.01	0.00	0.75	0.63	0.39	0.00
Na$_2$O	11.29	11.25	11.34	11.12	11.17	0.46	0.58	0.57	11.19	11.35	10.69	0.79
K$_2$O	0.13	0.09	0.08	0.10	0.07	16.11	16.03	15.69	0.07	0.06	0.09	11.30
MnO	0.03	0.00	0.00	0.00	0.05	0.07	0.00	0.03	0.02	0.01	0.00	0.03
TiO$_2$	0.04	0.00	0.00	0.00	0.00	0.01	0.06	0.00	0.00	0.00	0.00	0.01
Total	98.15	98.21	98.30	99.12	99.29	98.83	98.54	98.31	99.51	99.23	98.85	98.79
Number of ions based on 8 O												
Si	3.07	3.06	3.05	3.03	3.05	3.07	3.09	3.07	3.03	3.02	3.06	3.04
Al	0.88	0.90	0.92	0.93	0.92	0.89	0.88	0.90	0.94	0.94	0.92	1.03
Fe	0.97	0.97	0.98	0.95	0.95	0.04	0.05	0.05	0.95	0.97	0.91	0.00
Mg	0.00	0.00	0.00	0.00	0.00	0.00	0.00	0.00	0.00	0.00	0.00	0.00
Ca	0.02	0.03	0.03	0.05	0.02	0.00	0.00	0.00	0.04	0.03	0.02	0.00
Na	0.00	0.00	0.00	0.00	0.00	0.00	0.00	0.00	0.00	0.00	0.00	0.07
K	0.00	0.00	0.00	0.00	0.00	0.00	0.00	0.00	0.00	0.00	0.00	0.65
Mn	0.00	0.00	0.00	0.00	0.00	0.00	0.00	0.00	0.00	0.00	0.00	0.00
Ti	0.00	0.00	0.00	0.00	0.00	0.00	0.00	0.00	0.00	0.00	0.00	0.00
Mol.%An	2.02	2.52	2.54	4.56	2.29	0.00	0.04	0.00	3.56	2.95	1.96	0.00
Mol.%Ab	97.26	97.00	97.01	94.90	97.31	4.12	5.23	5.20	96.06	96.72	97.53	9.65
Mol.%Or	0.73	0.48	0.45	0.54	0.41	95.88	94.72	94.80	0.38	0.34	0.51	90.35

Table 8 Mineral chemical analyses of feldspar in equigranular granite from Pilok area

Sample	PL3-1-3				PL4-2-2				
SiO_2	69.80	69.11	69.18	67.49	69.12	69.31	67.06	67.25	66.96
Al_2O_3	18.05	18.17	18.14	17.95	18.29	17.67	17.82	17.76	17.85
FeO_{Total}	0.00	0.00	0.00	0.09	0.00	0.00	0.00	0.06	0.11
MgO	0.00	0.00	0.00	0.02	0.00	0.00	0.00	0.01	0.01
CaO	0.30	0.68	0.70	0.36	0.80	0.52	0.39	0.40	0.39
Na_2O	12.79	12.58	13.68	13.81	13.31	11.42	13.27	13.49	13.68
K_2O	0.14	0.13	0.08	0.06	0.12	0.08	0.08	0.08	0.12
MnO	0.00	0.01	0.02	0.00	0.02	0.00	0.00	0.05	0.01
TiO_2	0.00	0.00	0.00	0.00	0.00	0.00	0.00	0.00	0.00
Total	101.08	100.69	101.80	99.77	101.66	99.00	98.61	99.10	99.11
Number of ions based on 8 O									
Si	3.02	3.00	3.00	2.99	3.00	3.05	3.00	3.00	2.98
Al	0.92	0.93	0.93	0.94	0.93	0.92	0.94	0.93	0.94
Fe	1.07	1.06	1.15	1.18	1.12	0.97	1.15	1.16	1.18
Mg	0.00	0.00	0.00	0.00	0.00	0.00	0.00	0.00	0.00
Ca	0.01	0.03	0.03	0.02	0.04	0.02	0.02	0.02	0.02
Na	0.00	0.00	0.00	0.00	0.00	0.00	0.00	0.00	0.00
K	0.00	0.00	0.00	0.00	0.00	0.00	0.00	0.00	0.00
Mn	0.00	0.00	0.00	0.00	0.00	0.00	0.00	0.00	0.00
Ti	0.00	0.00	0.00	0.00	0.00	0.00	0.00	0.00	0.00
Mol.%An	1.26	2.86	2.75	1.40	3.19	2.45	1.60	1.61	1.54
Mol.%Ab	98.04	96.46	96.88	98.30	96.22	97.13	98.03	98.01	97.91
Mol.%Or	0.70	0.68	0.38	0.30	0.59	0.43	0.37	0.38	0.55

Table 9 *Mineral chemical analyses of feldspar grains in porphyritic granite and equigranular granite from Takua Pit Tong.*

Sample	TK1-1-5								TK4-1-4								
SiO_2	67.28	67.85	67.97	67.14	66.85	69.65	69.70	67.29	67.03	67.33	67.06	69.50	69.87	69.18	69.80	69.45	69.52
Al_2O_3	19.22	18.80	18.78	18.27	18.13	17.66	17.40	18.44	19.48	19.67	19.78	17.53	17.63	17.77	17.95	17.37	17.91
FeO	0.01	0.04	0.00	0.04	0.00	0.02	0.00	0.01	0.00	0.05	0.03	0.00	0.00	0.03	0.01	0.02	0.06
MgO	0.00	0.01	0.02	0.00	0.03	0.02	0.00	0.00	0.00	0.00	0.00	0.00	0.00	0.01	0.00	0.00	0.00
CaO	0.00	0.01	0.10	0.48	0.57	0.59	0.42	0.86	0.04	0.04	0.18	0.56	0.29	0.68	0.62	0.52	0.52
Na_2O	0.66	0.64	0.12	13.93	13.51	10.05	10.45	13.72	0.41	0.53	0.54	11.28	12.19	11.00	11.57	11.74	12.82
K_2O	11.71	11.11	11.09	0.09	0.15	0.15	0.10	0.14	11.76	11.27	11.81	0.09	0.09	0.06	0.08	0.07	0.14
MnO	0.01	0.00	0.03	0.00	0.00	0.00	0.03	0.03	0.05	0.04	0.01	0.01	0.01	0.00	0.00	0.02	0.00
TiO_2	0.00	0.00	0.01	0.00	0.00	0.00	0.00	0.00	0.00	0.03	0.00	0.00	0.00	0.00	0.01	0.01	0.00
Total	98.89	98.47	98.12	99.95	99.23	98.14	98.11	100.48	98.77	98.96	99.40	98.97	100.07	98.73	100.03	99.20	100.96
Number of ions based on 8 O																	
Si	3.05	3.07	3.08	2.97	2.97	3.08	3.08	2.96	3.04	3.04	3.02	3.05	3.05	3.05	3.04	3.06	3.02
Al	1.03	1.00	1.00	0.95	0.95	0.92	0.91	0.96	1.04	1.05	1.05	0.91	0.91	0.92	0.92	0.90	0.92
Fe	0.00	0.00	0.00	0.00	0.00	0.00	0.00	0.00	0.00	0.00	0.00	0.00	0.00	0.00	0.00	0.00	0.00
Mg	0.00	0.00	0.00	0.00	0.00	0.00	0.00	0.00	0.00	0.00	0.00	0.00	0.00	0.00	0.00	0.00	0.00
Ca	0.00	0.00	0.01	0.02	0.03	0.03	0.02	0.04	0.00	0.00	0.01	0.03	0.01	0.03	0.03	0.02	0.02
Na	0.06	0.06	0.01	1.19	1.17	0.86	0.90	1.17	0.04	0.05	0.05	0.96	1.03	0.94	0.98	1.00	1.08
K	0.68	0.64	0.64	0.00	0.00	0.00	0.00	0.00	0.68	0.65	0.68	0.00	0.00	0.00	0.00	0.00	0.00
Mn	0.00	0.00	0.00	0.00	0.00	0.00	0.00	0.00	0.00	0.00	0.00	0.00	0.00	0.00	0.00	0.00	0.00
Ti	0.00	0.00	0.00	0.00	0.00	0.00	0.00	0.00	0.00	0.00	0.00	0.00	0.00	0.00	0.00	0.00	0.00
Mol.%An	0.00	0.06	0.76	1.87	2.26	3.13	2.18	3.33	0.25	0.26	1.15	2.67	1.28	3.29	2.86	2.37	2.17
Mol.%Ab	7.84	8.07	1.55	97.69	97.05	95.96	97.22	96.04	4.98	6.67	6.38	96.83	98.24	96.38	96.72	97.28	97.13
Mol.%Or	92.16	91.87	97.69	0.43	0.69	0.91	0.61	0.63	94.77	93.07	92.47	0.50	0.47	0.33	0.42	0.35	0.70

2. <u>Tourmaline</u>

Tourmaline grains in equigranular granite from Pilok and Takua Pit Thong were analyzed and presented in Table 10 and Table 11, respectively. General chemical formula of tourmaline is $XY_3Z_6(T_6O_{18})(BO_3)_3V_3W$ where **X** are Na^+, K^+, Ca^{2+}, and vacancy; **Y** are Fe^{2+}, Mg^{2+}, Mn^{2+}, Al^{3+}, Li^+, Fe^{3+}, and Cr^{3+}; **Z** are Al^{3+}, Fe^{3+}, Mg^{2+}, and Cr^{3+}; **T** are Si^{4+}, Al^{3+}, and B^{3+}; **V** are OH^- and O^{2-}; and **W** are OH^-, F^-, and O^{2-} (Henry et al., 2011). Henry et al. (2011) recommended fixing Y+Z+T cations as a normalization method. However, Si was overestimated and exceed 6 atoms per formula unit (apfu). So, fixing Si atom was used as an alternative normalization method, where Si = 6 apfu.

Based on atom occupation in X-site and W site, all samples were classified as Alkali group (Figure 34a) and Hydroxy- species (Figure 34b), respectively. Note that X-site vacancy and H^+ cannot be analyzed by the microprobe, so, the estimation must be done. X-site vacancy was estimate by sum up the deficiency in the X-site, whereas H^+ was estimate by charge balance (Henry et al., 2011). In addition, all tourmaline samples were further classified into alkali-subgroup 1 based on major atom occupation in X-site and Li content (Figure 34c-d). Note that Li^+ was not measured and was estimated by sum up the deficiency in Y-site. Finally, based on major atom occupation in Y-site, i.e. Fe^{2+}, Mg^{2+}, and $2Li^+$, all tourmaline grains were classified as schorl (Figure 34e). Even though tourmaline from both Pilok and Takua Pit Thong was classified as schorl, the chemical composition does show the difference between the two places. Tourmaline in equigranular granite from Pilok area has lower X-site vacancy and Li^+, ranging from 0 to 0.035 apfu and 0.159 to 0.741 apfu, respectively, than those from Takua Pit Thong which are ranging from 0.202 to 0.317 apfu and 0.658 to 0.793 apfu, respectively (Figure 34e).

Table 10 Mineral chemical analyses of tourmaline in equigranular granite from Pilok.

Sample No.	PL3-1-1						PL4-2-1	
SiO_2	33.89	33.91	34.13	34.56	33.65	33.90	35.75	35.51
Al_2O_3	28.58	28.77	28.73	28.49	28.37	28.28	27.71	27.91
CaO	0.43	0.42	0.61	0.47	0.44	0.40	0.32	0.30
FeO_{Total}	16.72	16.29	15.75	15.99	15.78	16.38	15.16	15.51
Na_2O	2.70	2.75	2.74	2.57	2.76	2.68	2.76	2.77
K_2O	0.06	0.06	0.06	0.06	0.06	0.06	0.06	0.03
MnO	0.31	0.19	0.22	0.26	0.29	0.26	0.44	0.39
MgO	0.98	1.15	1.42	1.17	1.10	1.03	2.31	2.33
Cr_2O_3	0.00	0.04	0.05	0.00	0.00	0.00	0.00	0.08
TiO2	0.73	0.41	0.52	0.58	0.95	0.51	0.07	0.01
Y_2O_3	0.02	0.02	0.01	0.07	0.03	0.05	0.00	0.07
Total[1]	84.43	84.00	84.22	84.22	83.42	83.55	84.58	84.91
Number of ions based on 6 Si								
T site: Si	6.00	6.00	6.00	6.00	6.00	6.00	6.00	6.00
Z site: Al	5.96	6.00	5.95	5.83	5.96	5.90	5.48	5.56
Fe^{3+}	0.00	0.00	0.00	0.00	0.00	0.00	0.00	0.00
Cr^{3+}	0.00	0.00	0.01	0.00	0.00	0.00	0.00	0.01
Y^{3+}	0.00	0.00	0.00	0.00	0.00	0.00	0.00	0.00
Mg^{2+}	0.04	0.00	0.04	0.17	0.04	0.10	0.52	0.43
Fe^{2+}	0.00	0.00	0.00	0.00	0.00	0.00	0.00	0.00
Z-site Total	6.00	6.00	6.00	6.00	6.00	6.00	6.00	6.00
Y site: Al	0.00	0.00	0.00	0.00	0.00	0.00	0.00	0.00
Ti	0.10	0.05	0.07	0.08	0.13	0.07	0.01	0.00
Fe^{3+}	0.00	0.00	0.00	0.00	0.00	0.00	0.00	0.00
Fe^{2+}	2.48	2.41	2.32	2.32	2.35	2.43	2.13	2.19
Mn^{2+}	0.05	0.03	0.03	0.04	0.04	0.04	0.06	0.06
Mg^{2+}	0.22	0.30	0.33	0.13	0.25	0.17	0.06	0.16
Li^+	0.16	0.21	0.25	0.43	0.22	0.30	0.74	0.60
Y-site Total	3.00	3.00	3.00	3.00	3.00	3.00	3.00	3.00

[1]SIMS were not performed to measure B, Li, and H value, resulting in below 100% total

Table 10 Mineral chemical analyses of tourmaline in equigranular granite from Pilok

Sample No.	PL3-1-1						PL4-2-1	
X site: Ca	0.08	0.08	0.11	0.09	0.08	0.08	0.06	0.05
Na	0.93	0.94	0.93	0.86	0.95	0.92	0.90	0.91
K	0.01	0.01	0.01	0.01	0.01	0.01	0.01	0.01
x$\square$	0.00	0.00	0.00	0.03	0.00	0.00	0.03	0.03
X-site Total	1.02	1.04	1.06	1.00	1.05	1.01	1.00	1.00
X-site primary group:	Alkali	Alkali	Alkali	Alkali	Alkali	Alkali	Alkali	Alkali
W-site species series:	Hydroxy	Hydroxy	Hydroxy	Hydroxy	Hydroxy	Hydroxy	Hydroxy	Hydroxy
V-site dominant cation:	OH	OH	OH	OH	OH	OH	OH	OH
Dominant $^{Z}R^{3+}$	Al^{3+}	Al^{3+}	Al^{3+}	Al^{3+}	Al^{3+}	Al^{3+}	Al^{3+}	Al^{3+}
Dominant $^{Y}R^{2+}$	Fe^{2+}	Fe^{2+}	Fe^{2+}	Fe^{2+}	Fe^{2+}	Fe^{2+}	Fe^{2+}	Fe^{2+}
Dominant $^{Y}R^{3+}$	-	-	-	-	-	-	-	-
$Ca^{2+}/(Ca^{2+}+Na^{+}+K^{+})$	0.08	0.08	0.11	0.09	0.08	0.08	0.06	0.06
$^{X}\square/^{X}\square+Na^{+}+K^{+}$	0.00	0.00	0.00	0.04	0.00	0.00	0.03	0.04
$^{YZ}R^{2+}/^{YZ}R^{2+}+2Li^{+}$	0.90	0.87	0.85	0.76	0.86	0.82	0.65	0.71
Subgroup	sub-group 1	sub-group 1	sub-group 1	sub-group 1	sub-group 1	sub-group 1	sub-group 1	sub-group 1
Tourmaline species	Schorl	Schorl	Schorl	Schorl	Schorl	Schorl	Schorl	Schorl

Table 11 Mineral chemical analyses of tourmaline in equigranular granite from Takua Pit Thong

Sample No.	TK4-1-4				
SiO_2	35.35	35.45	36.06	35.38	34.89
Al_2O_3	29.26	29.24	30.18	28.74	28.99
CaO	0.29	0.30	0.25	0.22	0.25
TiO_2	0.87	0.95	0.54	0.85	0.85
MgO	1.23	1.28	2.39	1.38	1.39
Na_2O	2.22	2.22	1.95	2.11	2.18
K_2O	0.02	0.06	0.04	0.03	0.04
FeO_{Total}	14.66	14.54	12.61	14.68	14.41
BaO	0.02	0.07	0.00	0.04	0.03
MnO	0.37	0.34	0.12	0.22	0.25
Total[1]	84.30	84.43	84.15	83.64	83.29
Number of ions based on 6 Si					
T site: Si	6.00	6.00	6.00	6.00	6.00
Z site: Al	5.85	5.83	5.92	5.75	5.88
Fe^{3+}	0.00	0.00	0.00	0.00	0.00
Mg^{2+}	0.15	0.17	0.08	0.25	0.12
Fe^{2+}	0.00	0.00	0.00	0.00	0.00
Z-site Total	6.00	6.00	6.00	6.00	6.00
Y site: Al	0.00	0.00	0.00	0.00	0.00
Ti	0.11	0.12	0.07	0.11	0.11
Fe^{2+}	2.08	2.06	1.75	2.08	2.07
Mn	0.05	0.05	0.02	0.03	0.04
Mg	0.03	0.03	0.06	0.03	0.03
Li	0.70	0.74	0.72	0.79	0.66
Y-site Total	2.98	3.00	2.62	3.05	2.91

[1]SIMS were not performed to measure B, Li, and H value, resulting in below 100% total

Table 11 Mineral chemical analyses of tourmaline in equigranular granite from Takua Pit Thong

Sample No.	TK4-1-4				
X-site: Ca	0.05	0.06	0.04	0.04	0.05
Na	0.73	0.73	0.63	0.69	0.73
K	0.00	0.01	0.01	0.01	0.01
$^x\square$	0.21	0.20	0.32	0.26	0.22
X-site Total	1.00	1.00	1.00	1.00	1.00
X-site primary group:	Alkali	Alkali	Alkali	Alkali	Alkali
W-site species series:	Hydroxy	Hydroxy	Hydroxy	Hydroxy	Hydroxy
V-site dominat cation:	OH	OH	OH	OH	OH
Dominant $^ZR^{3+}$	Fe^{2+}	Fe^{2+}	Fe^{2+}	Fe^{2+}	Fe^{2+}
Dominant $^YR^{2+}$	-	-	-	-	-
Dominant $^YR^{3+}$	Al^{3+}	Al^{3+}	Al^{3+}	Al^{3+}	Al^{3+}
$Ca^{2+}/(Ca^{2+}+Na^++K^+)$	0.07	0.07	0.07	0.05	0.06
$^x\square/^x\square+Na^++K^+$	0.23	0.21	0.33	0.27	0.23
$^{YZ}R^{2+}/^{YZ}R^{2+}+2Li^+$	0.64	0.62	0.62	0.61	0.65
Subgroup	subgroup 1	subgroup 2	subgroup 3	subgroup 4	subgroup 5
Tourmaline species	Schorl	Schorl	Schorl	Schorl	Schorl
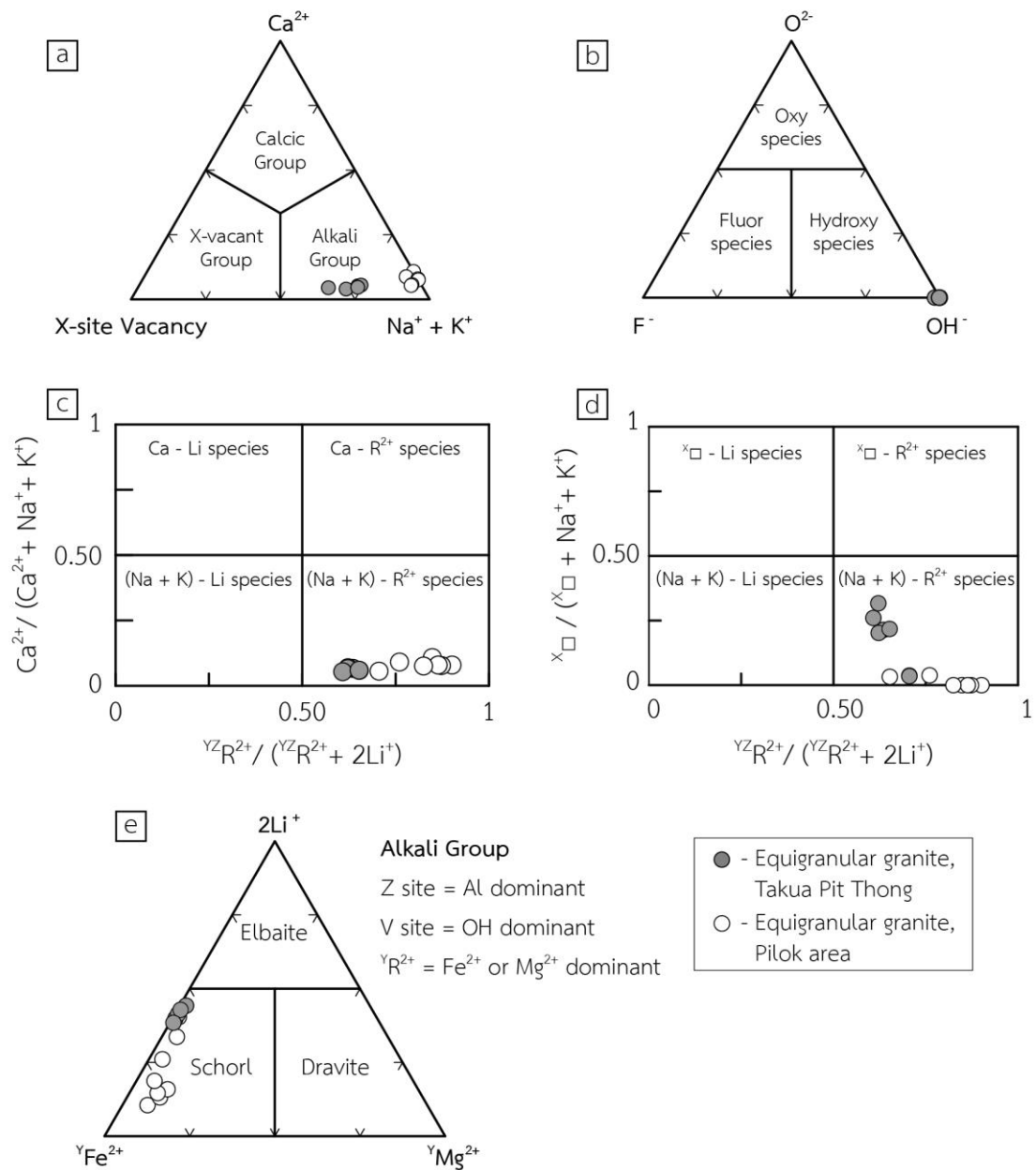
Figure 34 Plot of mineral chemistry for tourmaline (Henry et al., 2011): (a) Ternary system for the primary tourmaline group based on the dominant occupancy at the X site; (b) Ternary system for a general series of tourmaline species based on the anion occupancy at the W site; (c) Determination of subgroup 1 – 4 for alkali- and calcic Tourmalines, plotting $Ca^{2+}/(Ca^{2+}+Na^++K^+)$ against $^{YZ}R^{2+}/(^{YZ}R^{2+}+2Li^+)$ and considering the dominant anion at W site; (d) Determination of subgroup 1 – 4 for alkali- and X-vacant-group tourmalines, plotting a value of $^X\square/(^X\square+Na^++K^+)$ against $^{YZ}R^{2+}/(^{YZ}R^{2+}+2Li^+)$ and considering the dominant anion at W site; and (e) Ternary diagram for classifying alkali-group tourmaline species with Al^{3+} dominance at Z site and OH dominance at V site, respectively. It plotted Y-site cations on the ternary diagram and revealed tourmaline specie.

CHAPTER V

DISCUSSION AND CONCLUSION

Petrogenesis

Based on macroscopic and microscopic studies of granitic rocks in Pilok and Takua Pit Thong areas, porphyritic granite and equigranular granite have felsic composition which are classified as alkali feldspar granite, syenogranite, and monzogranite (Figure 17). This modal classification suggest that granites can be either continental epeirogenic uprift granite (CEUG) which is considered anorogenic granite, or post-orogenic granite (POG) and continental collision granite (CCG) which are considered orogenic granite (Maniar and Piccoli, 1989).

Geochemically, Al_2O_3 and K_2O of both porphyritic granite and equigranular granite from both areas have a narrow composition range and irregular correlation against SiO_2 (Figure 24a and Figure 24h). This should be due to the high mobility characteristics of Al and K (Cox et al., 1979). In addition, plots between SiO_2 and K_2O (Figure 24h and Figure 35a) can still be used to interpreted that these granites are not oceanic plagiogranite (OP) (Maniar and Piccoli, 1989). In addition, plots of SiO_2 vs. Fe* (Figure 25a and Figure 35c) show a wide distribution ranging from ferroan rock to magnesian rock which cannot be used to classified if they are orogenic granite or anorogenic granite (Maniar and Piccoli, 1989). However, this assumption, together with relationship of SiO_2 and Al_2O_3 (Figure 35b) can be used to interpret that both granites are post-orogenic granite (POG) (Maniar and Piccoli, 1989). Furthermore, ASI plots (Figure 25c) which are indicating that all granites are peraluminous rock (Shand, 1943; Frost et al., 2001) and their S-type affinity suggest that they are continental collision granites (CAG), a result of sedimentary rock anatexis.

To support the assumption, a Hf-Rb-Ta ternary diagram (Harris, Pearce, and Tindle, 1986) was used to interpreted the petrogenesis of the granites. As a result, most of the plot fell in group III or post-collision region (Figure 36), which support the assumption.
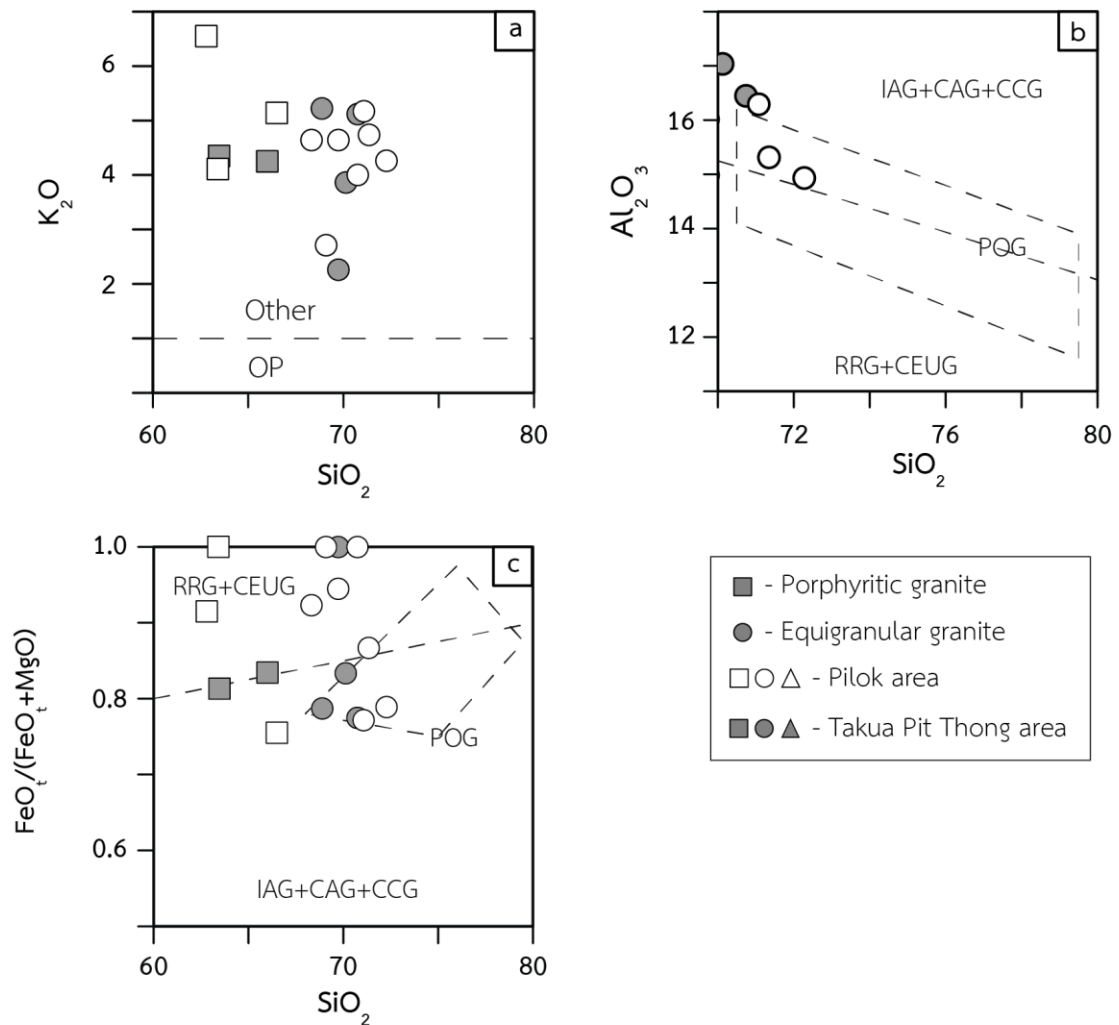
Figure 35 Tectonic discrimination diagram (Maniar and Piccoli, 1989): (a) plots of SiO2 vs. K2O, discriminating OP from others; (b) plots of SiO2 vs. Al2O3, divided the plot into 3 group: RRG+CEUG, IAG+CAG+CCG, and POG; and (c) plots of SiO2 vs. Fe*. Abbreviations are: OP = Oceanic Plagiogranite, RRG = Rift-related granite, CEUG = Continental epeirogenic uprift granite, IAG = Island arc granite, CAG = Continental arc granite, CCG = Continental collision granite, and POG = Post-orogenic granite.
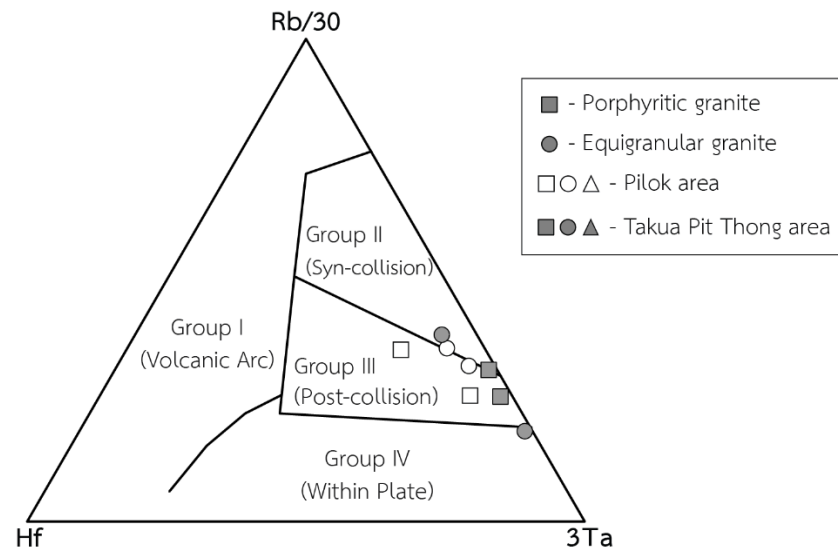
Figure 36 Hf-Rb-Ta ternary diagram (Harris et al., 1986) of porphyritic granite and equigranular granite from Pilok and Takua Pit Thong.
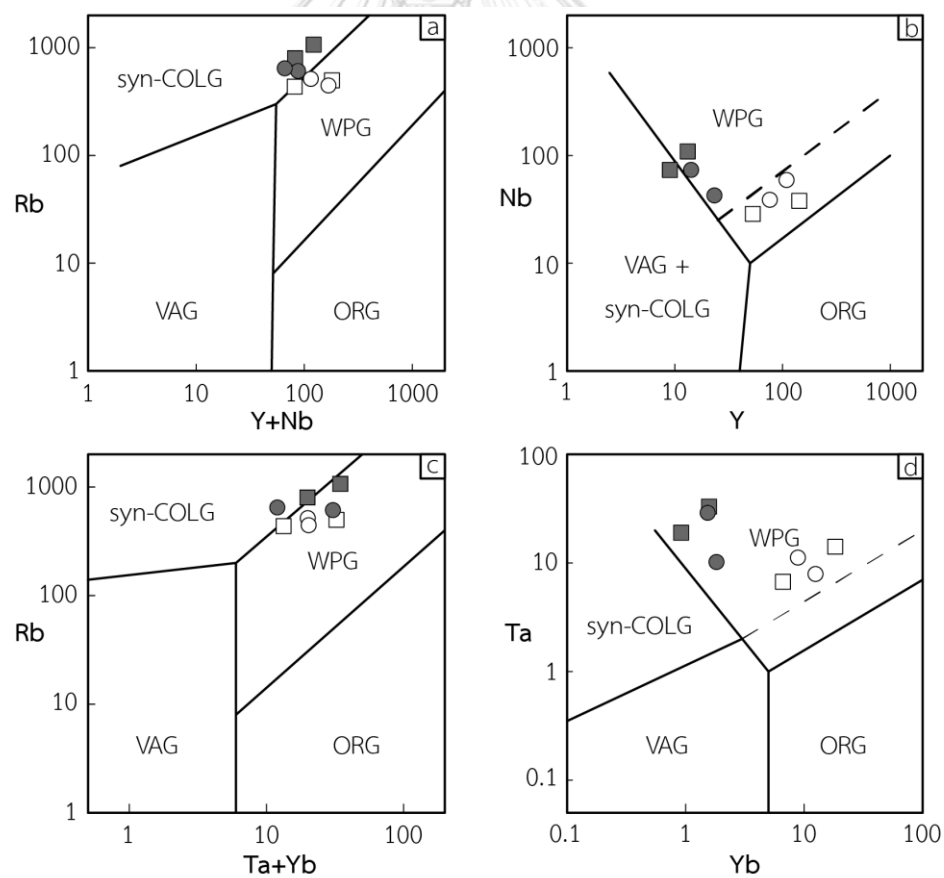
Figure 37 Immobile elements plots (after Pearce, Harris, and Tindle, 1984) of porphyritic granite and equigranular granite from Pilok and Takua Pit Thong area: (a) Rb vs. Y+Nb; (b) Nb vs. Y; (c) Rb vs. Ta+Yb; and (d) Ta vs. Yb. Rock type symbols are as same as in Figure 36

As for trace element and REE of porphyritic granite and equigranular granite from both areas, they are enriched in U, Th, and Pb, which are typical for felsic magma derivation (Wilson, 1989). In addition, the enrichment of LILE imply the late-stage magma of both granites (Figure 26a, c). Trace element plots (after Pearce et al., 1984) of Y vs. Nb (Figure 37b) and Yb vs. Ta (Figure 37d) indicate that both granites are tectonically classified as within-plate granite (WPG). In addition, plots of Y+Nb vs. Rb (Figure 37a) and Ta+Yb vs. Rb (Figure 37c) lies at the boundary of syn-collision granite (syn-COLG) and within-plate granite (WPG). Furthermore, plots from these four diagrams lies close the boundaries of volcanic arc granite (VAG), syn-COLG, and WPG, but do not fall in ORG field. This phenomenon is typical for post-collision granite which is affected from melting of the lower crust and melting of the upper mantle (Pearce et al., 1984; Harris et al., 1986; Pearce, 1996).

Considering all the above, porphyritic granite and equigranular granite are interpreted as post-collisional granite (Harris et al., 1986), which is one of post-orogenic event (Pearce, 1996).

Tectonic Implication

As discussed in the previous topic, the petrogenetic condition of Pilok and Takua Pit Thong is a post-collision event, an anatexis of sedimentary host rock. But, without the geochronological data, the tectonic evolution is hard to interpret. However, using geotectonic assumption from previous studies in mainland Southeast Asia (Bunopas, 1981; Bunopas and Vella, 1983; Cobbing et al., 1986; Cobbing et al., 1992; Charusiri et al., 1993; Schwartz et al., 1995; Charusiri et al., 2002; Cobbing, 2011; Khin Zaw et al., 2014; Wang et al., 2014), and the fact that both areas are located at the margin of Sibumasu Terrane and Western Myanmar Terrane, it can be inferred that both granites are resulted from the collision of Sibumasu Terrane and Western Myanmar Terrane in Cretaceous to Miocene (Charusiri et al., 1993).

A Comparison Between Pilok and Takua Pit Thong Deposits

Even though granites from both areas are very similar in composition. However, some difference can be observed. Geochemically, granites from Pilok area has slightly high alkali content than granites from Takua Pit Thong area especially Na_2O and K_2O. Regarding to mineral chemistry, some differences in Tourmaline have been observed in which tourmaline of equigranular granite from Takua Pit Thong area has higher X-site vacancy and Li content in Y-site. This granite could be a potential source for lithium resources.

Table 12 A comparison chart of geological and mineralogical characteristics of Pilok and Takua Pit Thong Tin-tungsten deposits

List	Pilok	Takua Pit Thong
Granite facies	2 units: porphyritic granite and equigranular granite	
Fe*	Ferroan to Magnesian	
MALI	Alkalic rock and Alkalic to alkali-calcic rock	
Fsp Chemistry	Same	
ASI	Peraluminous, less ASI	Peraluminous, more ASI
Tur Chemistry	Lower Li and X-site vacancy	Higher Li and X-site vacancy
I-, S-type	S-type	
Trace element	LILE and HFSE enrichment	
REE	More LREE and less HREE	
Tectonic Setting	Post-collision intrusion	
Magma Source	Lower Crust & upper mantle melting	
Tectonic Event	Collision of Western Burma Terrane & Sibumasu Terrane	

Conclusion

Granitic rocks from Pilok and Takua Pit Thong area can be classified into two units: porphyritic granite and equigranular granite. Major and minor oxides of the two units of granite revealed that porphyritic granite is ferroan to magnesian, alkalic, peraluminous rock, whereas equigranular granite is ferroan to magnesian, alkali-calcic, peraluminous rock. In addition, LILE and mineral assemblages suggest the late stage of magma evolution for both porphyritic granite and equigranular granite. Furthermore, the peraluminous characteristic, the S-type affinity, enrichment of LILE and HFSE, and the trace element characteristic of both porphyritic granite and equigranular granite from Pilok and Takua Pit Thong area are originated from anatexis of sedimentary rock, resulting from post-collision event between Western Myanmar Terrane in the west and Sibumasu Terrane in the east. Tourmaline and feldspar chemistry show typical composition for granite and support the petrogenesis idea, however, a slightly high concentration of lithium in tourmaline from Pilok is noted here.

Suggestion

Since both areas are heavily altered and weathered, more samples from another area in the same belt which are fresh should be add to the petrochemistry analysis to confirm the contradiction of the data. In addition, a geochronology would complete the tectonic evolution implementation from this work.

REFERENCES

Ali, J., Cheung, H. M. C., Aitchison, J. C., and Sun, Y. 2013. Palaeomagnetic re-investigation of Early Permian rift basalts from the Baoshan Block, SW China: constraints on the site-of-origin of the Gondwana-derived eastern Cimmerian terranes. Geophysical Journal International 193(2): 650-663.

Altermann, W. 1986. The Upper Palaeozoic pebbly mudstone facies of Peninsular Thailand and Western Malaya - Continental margin deposits of Palaeoeurasia. Geologische Rundschau 75: 371-381.

Ampaiwan, T., Hisada, K., and Charusiri, P. 2009. Lower Permian glacially influenced deposits in Phuket and adjacent islands, peninsular Thailand. Island Arc 18(1): 52-68.

Archbold, N. W., Pigram, C. J., Ratman, N., and Hakim, S. 1982. Indonesian Permian brachiopod fauna and Gondwana–South-East Asia relationships. Nature 296(5857): 556-558.

Barber, A. J., and Crow, M. J. 2009. Structure of Sumatra and its implications for the tectonic assembly of Southeast Asia and the destruction of Paleotethys. Island Arc 18(1): 3-20.

Barr, S. M., and Macdonald, A. S. 1991. Toward a late Palaeozoic-early Mesozoic tectonic model for Thailand. Journal of Thai Geosciences 1: 11-22.

Blevin, P. L., and Chappell, B. W. 1995. Chemistry, origin, and evolution of mineralized granites in the Lachlan fold belt, Australia: the metallogeny of I- and S-type granite. Economic Geology 90: 1604-1619.

Boynton, W. V. 1984. Cosmochemistry of the rare earth elements: meteorite studies. In P. Henderson (ed.), Rare Earth Element Geochemistry, vol. 2. Developments in Geochemistry. pp. 63-114. Amsterdam: Elsevier.

Brown, G. F., Buravas, S., Charaljavanaphet, J., Jalichandra, N., Johnston, W. D., Sethaputra, V., and Taylor, G. C. 1951. Geologic reconnaissance of the mineral deposits of Thailand. vol. 984. U.S. Geological Survey Bulletin. Washington: United States Government Printing Office.

Bunopas, S. 1981. Paleogeographic history of Western Thailand and adjacent parts of South-east Asia. Doctoral dissertation. Victoria University of Wellington.

Bunopas, S., and Vella, P. 1983. Tectonic and geologic evolution of Thailand. In P. Nutalaya (ed.), Proceedings of a workshop on stratigraphic correlation of Thailand and Malaysia, pp. 307-322. Bangkok: Geological Society of Thailand.

Bunopas, S., and Vella, P. 1989. Palaeozoic and Early Mesozoic rotation and drifting of Shan-Thai from Gondwana-Australia. 4th International Symposium on preJurassic evolution of East Asia, IGCP Project 224, Reports and Abstracts 1: 63-64.

Bureau of Geology and Mineral Resources of Yunnan. 1990. Regional geology of the Yunnan province. Beijing: Geological Publishing House. [in Chinese]

Burrett, C., Long, J., and Stait, B. 1990. Early-Middle Palaeozoic biogeography of Asian terranes derived from Gondwana. Geological Society, London, Memoirs 12(1): 163-174.

Burrett, C., and Stait, B. 1985. South East Asia as a part of an Ordovician Gondwanaland—a palaeobiogeographic test of a tectonic hypothesis. Earth and Planetary Science Letters 75(2): 184-190.

Burrett, C., Zaw, K., Meffre, S., Lai, C. K., Khositanont, S., Chaodumrong, P., Udchachon, M., Ekins, S., and Halpin, J. 2014. The configuration of Greater Gondwana—Evidence from LA ICPMS, U–Pb geochronology of detrital zircons from the Palaeozoic and Mesozoic of Southeast Asia and China. Gondwana Research 26: 31-51.

Chaodumrong, P. 2010. Revised Lithostratigraphy of the Kaeng Krachan Group. Lithostratigraphy standard academic report No. 1/2553. Bangkok: Department of Mineral Resources.

Chaodumrong, P., Assavapatchara, S., and Jongautchariyakul, S. 2004. Comparative research on Permian strata and fauna between West Yunnan and West Thailand. Completed research report on cooperation with foreign countries (Thailand - China). Bangkok: National Research Council of Thailand. [in Thai with English abstract]

Chappell, B. W., and White, A. J. R. 1974. Two contrasting granite types. Pacific

Geology 8: 173-174.

Charusiri, P. 1989. Lithophile metallogenic epochs of Thailand: A geological and geochronological investigation. Doctoral dissertation. Queen's University.

Charusiri, P., Clark, A. H., Farrar, E., Archibald, D., and Charusiri, B. 1993. Granite belts in Thailand: evidence from the ^{40}Ar/^{39}Ar geochronological and geological syntheses. Journal of Southeast Asian Earth Sciences 8(1): 127-136.

Charusiri, P., Daorerk, V., Archibald, D., Hisada, K., and Ampaiwan, T. 2002. Geotectonic Evolution of Thailand : A New Synthesis. Journal of Geological Society of Thailand 1: 1-20.

Cobbing, E. J. 2011. Granitic rocks. In M. F. Ridd, A. J. Barber, and M. J. Crow (eds.), The Geology of Thailand, pp. 441-458. London: Geological Society.

Cobbing, E. J., Mallick, D. I. J., Pitfield, P. E. J., and Teoh, L. H. 1986. The granites of the Southeast Asian Tin Belt. Journal of the Geological Society 143(3): 537-550.

Cobbing, E. J., Pitfield, P. E. J., Derbyshire, D. P. F., and Mallick, D. I. J. 1992. The granites of the South-East Asian tin belt. vol. 10. Overseas Memoir of the British Geological Survey. London: British Geological Survey.

Cox, K. G., Bell, J. D., and Pankhurst, R. J. 1979. The Interpretation of Igneous Rocks. Dordrecht: Springer Netherlands.

Craig, J. R., and Vaughan, D. J. 1994. Ore Microscopy and Ore Petrography. 2nd ed. New York: John Wiley & Sons.

Darbyshire, D. P. F., and Swainbank, I. G. 1988. South-east Asia Granite Project: Geochronology of a selection of granites from Burma. National Environment Research Council, Isotope Geology Centre Report No. 88/6.

Department of Highway. 2009. Highway Map Central Region[Highway Map]. Bangkok: Department of Highway.

Department of Mineral Resources. 2014. Geology of Thailand. Bangkok: Department of Mineral Resources.

Dheeradilok, P., Udomsrisuk, T., Tansuwan, V., Jungyusuk, N., and Nakanart, A. 1985. Changwat Nakhorn Pathom[Geological map]. Sheet ND47-11, Scale 1:250,000. Bangkok: Department of Mineral Resources.

ERSI. 2009. World Street Map[Online]. Available from:

https://www.arcgis.com/home/item.html?id=3b93337983e9436f8db950e38a8629af. [15 April 2020]

Fang, N., and Yang, W. 1991. A study of the oxygen and carbon isotope records from Upper Carboniferous to Lower Permian in Western Yunnan, China. In J. Ren, and G. Xie (eds.), Proceedings of First International Symposium on Gondwana Dispersion and Asian Accretion - Geological Evolution of Eastern Tethys, pp. 35-36. Beijing: China University of Geosciences.

Fang, W., Van der Voo, R., and Liang, Q. 1989. Devonian paleomagnetism of Yunnan Province across the Shan Thai-South China Suture. Tectonics 8(5): 939-952.

Fourcade, S., and Allegre, C. J. 1981. Trace elements behavior in granite genesis: A case study The calc-alkaline plutonic association from the Querigut complex (Pyrénées, France). Contributions to Mineralogy and Petrology 76: 177-195.

Frost, B. R., Barnes, C. G., Collins, W. J., Arculus, R. J., Ellis, D. J., and Frost, C. D. 2001. A geochemical classification for granitic rocks. Journal of petrology 42(11): 2033-2048.

Harker, A. 1909. The Natural History of Igneous Rocks. London: Methuen.

Harris, N. B. W., Pearce, J. A., and Tindle, A. G. 1986. Geochemical characteristics of collision-zone magmatism. Geological Society, London, Special Publications 19(1): 67-81.

Hennig, D., Lehmann, B., Frei, D., Belyatsky, B., Zhao, X. F., Cabral, A. R., Zeng, P. S., Zhou, M. F., and Schmidt, K. 2009. Early Permian seafloor to continental arc magmatism in the eastern Paleo-Tethys: U–Pb age and Nd–Sr isotope data from the southern Lancangjiang Zone, Yunnan, China. Lithos 113(3-4): 408-422.

Henry, D. J., Novák, M., Hawthorne, F. C., Ertl, A., Dutrow, B. l., Uher, P., and Pezzotta, F. 2011. Nomenclature of the tourmaline-supergroup minerals. American Mineralogist 96: 895-913.

Henry, D. J., Viator, D., and Dutrow, B. L. 2002. Estimation of light element concentrations in tourmaline: How accurate can it be? .Programme with Abstracts of the 18th International Mineralogical Association, p. 209. Edinburgh: International Mineralogical Assocciation.

Hills, J. W. 1989. The geology of Phuket district of Thailand and its tectonic

relationship to Gondwanaland. Honors Thesis. Department of Geology, University of Tasmania.

Horwitz, W. 1990. Nomenclature for sampling in analytical chemistry (Recommendations 1990). Pure and Applied Chemistry 62(6): 1193-1208. [in English]

Hosking, K. 1969. The nature of the primary tin ores of the south-west of England. Bangkok: International Tin Council.

Hosking, K. F. G. 1988. The world's major types of tin deposit. In C. S. Hutchison (ed.), Geology of Tin Deposits in Asia and the Pacific, pp. 3-49. Berlin: Springer-Verlag.

Huang, K., and Opdyke, N. D. 1991. Paleomagnetic results from the Upper Carboniferous of the Shan-Thai-Malay block of western Yunnan, China. Tectonophysics 192(3): 333-344.

Hutchison, C. S. 1977. Granite emplacement and tectonic subdivision of Peninsular Malaysia. Bulletin of the Geological Society of Malaysia 9: 187-207.

Ingavat, R., and Douglass, R. 1981. Fusuline fossils from Thailand, Part XIV: the fusulinid genus Monodiexodina from Northwest Thailand. Geology and Palaeontology of Southeast Asia 22: 23-34.

Irvine, T. N., and Baragar, W. R. A. 1971. A guide to the chemical classification of the common volcanic rocks. Canadian Journal of Earth Sciences 8(5): 523-548.

Janoušek, V., Farrow, C. M., and Erban, V. 2006. Interpretation of Whole-rock Geochemical Data in Igneous Geochemistry: Introducing Geochemical Data Toolkit (GCDkit). Journal of Petrology 47(6): 1255-1259.

Javanaphet, J. C. 1969. Geological map of Thailand[Geological map]. Scale 1:1,000,000. Bangkok: Department of Mineral Resources.

Jones, C. R. 1968. Lower Palaeozoic rocks of the Malay Peninsula. American Association of Petroleum Geologists Bulletin 52: 1259-1278.

Kemlheg, S., and Chiamton, S. 1989. Ban I Tong[Geological map]. Sheet 4638II, Scale 1:50,000. Bangkok: Department of Mineral Resources.

Khin Zaw, Meffre, S., Lai, C., Burrett, C., Santosh, M., Graham, I., Manaka, T., Salam, A., Kamvong, T., and Cromie, P. 2014. Tectonics and metallogeny of mainland Southeast Asia — A review and contribution. Gondwana Research 26(1): 5-30.

Lechler, P. J., and Desilets, M. O.   1987.   A review of the use of loss on ignition as a measurement of total volatiles in whole-rock analysis.   Chemical Geology 63(3): 341-344.

Leewongcharoen, S., and Chaturongkawanich, S.   1994.   Muang Thung Chedi Quadrangle[Geological map].   Sheet 4836III,   Scale 1:50,000.   Bangkok: Department of Mineral Resources,.

Lehmann, B., Jungyusuk, N., Khositanont, S., Höhndorf, A., and Kuroda, Y.   1994.   The tin-tungsten ore system of Pilok, Thailand.   Journal of Southeast Asian Earth Sciences 10: 51-63.

Li, G. Z., Su, S. G., Lei, W. Y., and Duan, X. D.   2011.   Precise ID-TIMS zircon U–Pb age and whole-rock geochemistry of the Nanlinshan mafic intrusion in the southern Lancangjiang arc terrane, Sangjiang area, SW China.   Earth Science Frontiers 18: 206-212. [in Chinese with English abstract]

Mahawat, C.   1988.   The geological characteristics of the Pilok Sn-W-Mo deposits, west Thailand.   In C. S. Hutchison (ed.), Geology of Tin Deposits in Asia and the Pacific, pp. 696-709.   New York: Springer-Verlag.

Maniar, P. D., and Piccoli, P. M.   1989.   Tectonic discrimination of granitoids.   Geological Society of America Bulletin 101(5): 635-643.

Materikov, M. P.   1977.   Deposits of Tin.   In V. I. Smirnov (ed.), Ore Deposits of the USSR, vol. 3. pp. 229-294.   London: Pitman.

Metcalfe, I.   1984.   Stratigraphy, palaeontology and palaeogeography of the Carboniferous of Southeast Asia.   Memoires de la Societe Geologique de France 147: 107-118.

Metcalfe, I.   1988.   Origin and assembly of south-east Asian continental terranes.   In M. G. Audley-Charles, and A. Hallam (eds.), Gondwana and Tethys, vol. 37. Geological Society Special Publications. pp. 101-118.   New York: Oxford University Press.

Metcalfe, I.   1991.   Late palaeozoic and mesozoic palaeogeography of Southeast Asia. Palaeogeography, Palaeoclimatology, Palaeoecology 87(1): 211-221.

Metcalfe, I.   1994.   Gondwanaland origin, dispersion, and accretion of East and Southeast Asian continental terranes.   Journal of South American Earth Sciences

7(3): 333-347.

Metcalfe, I.   2002.   Permian tectonic framework and palaeogeography of SE Asia. Journal of Asian Earth Sciences 20(6): 551-566.

Metcalfe, I.   2011.   Tectonic framework and Phanerozoic evolution of Sundaland. Gondwana Research 19(1): 3-21.

Metcalfe, I.   2013.   Gondwana dispersion and Asian accretion: Tectonic and palaeogeographic evolution of eastern Tethys.   Journal of Asian Earth Sciences 66: 1-33.

Metcalfe, I.   2017.   Tectonic evolution of Sundaland.   Bulletin of the Geological Society of Malaysia 63: 27-60.

Mitchell, A. H. G., Young, B., and Jautaranipa, W.   1970.   The Phuket Group, peninsular Thailand: a palaeozoic geosynclinal deposit.   Geological Magazine 107: 411-428.

Nie, F., Dong, G. C., Mo, X. X., Zhu, D. C., Dong, M. L., and Wang, X.   2012. Geochemistry, zircon U–Pb chronology of the Triassic granites in the Changning–Menglian suture zone and their implications.   Acta Petrologica Sinica 28: 1465–1476. [in Chinese with English abstract]

Pearce, J. A.   1996.   Sources and settings of granitic rocks.   Episodes 19: 120-125.

Pearce, J. A., Harris, N. B. W., and Tindle, A. G.   1984.   Trace element discrimination diagrams for the tectonic interpretation of granitic rocks.   Journal of Petrology 25: 956-983.

Piyasin, S.   1975.   Stratigraphy and sedimentology of the Kaeng Krachan Group (Carboniferous).   In R. B. Stokes, and C. Tantisukrit (eds.), Proceedings of the Conference on Geology of Thailand, pp. 25-35.   Chiang Mai: Department of Geological Sciences, Chiang Mai University.

Qin, Y. J.   1991.   Basic characteristics and tectonic emplacement mechanism of Lincang granite batholith in western Yunnan province, China.   Doctoral dissertation. Institute of Geology and Geophysics, Chinese Academy of Sciences. [in Chinese]

Raksaskulwong, L., and Wongwanich, T.   1993.   Stratigraphy of the Kaeng Krachan Group in Peninsular and Western Thailand.   Geological research report.   Bangkok: Geological Survey Division, Department of Mineral Resources. [in Thai]

Ridd, M. F.   2011.   Lower Palaeozoic.   In M. F. Ridd, A. J. Barber, and M. J. Crow (eds.),

The Geology of Thailand, pp. 33-52. London: Geological Society.

Schwartz, M. O., Rajah, S. S., Askury, A. K., Putthapiban, P., and Djaswadi, S. 1995. The Southeast Asian tin belt. Earth-Science Reviews 38(2): 95-293.

Şengör, A. M. C. 1979. Mid-Mesozoic closure of Permo–Triassic Tethys and its implications. Nature 279(5714): 590-593.

Şengör, A. M. C. 1984. The Cimmeride Orogenic System and the Tectonics of Eurasia. Geological Society of America Special Paper 195: 0.

Shand, S. J. 1943. Eruptive Rocks: Their Genesis, Composition, Classification, and their Relation to Ore-Deposits, with a Chapter on Meteorite. 2nd ed. New York: John Wiley & Sons.

Shi, L., Chen, J. C., Wu, S. L., Peng, X. J., and Tang, S. C. 1989. Metallogenic Regularity of Western Yunnan Sn Belt. Beijing: Geological Publishing House. [in Chinese]

Shi, M., Lin, F., Fan, W., Wang, H., Cong, F., and Zhu, H. 2015. SHRIMP zircon U-Pb dating of the monzogranites in the Pilok tin tungsten mining area, western Thailand, and its geological implications. Geological Bulletin of China 34(4): 769-779.

Shi, Y., Jin, X., Huang, H., and Yang, X. 2008. Permian fusulinids from the Tengchong Block, Western Yunnan, China. Journal of Paleontology 82(1): 118-127.

Siribhakdi, K., Salyapongse, S., and Suteetorn, V. 1985. Tavoy[Geological map]. Sheet ND47-6, Scale 1:250,000. Bangkok: Department of Mineral Resources.

Sone, M., and Metcalfe, I. 2008. Parallel Tethyan sutures in mainland Southeast Asia: New insights for Palaeo-Tethys closure and implications for the Indosinian orogeny. Comptes Rendus Geoscience 340(2): 166-179.

Stauffer, P. H., and Lee, C. P. 1989. Late Palaeozoic glacial marine facies in Southeast Asia and its implications. Bulletin of the Geological Society of Malaysia 20: 363-397.

Streckeisen, A. 1974. Classification and nomenclature of plutonic rocks recommendations of the IUGS subcommission on the systematics of igneous rocks. Geologische Rundschau 63(2): 773-786.

Sun, S.-s., and McDonough, W. F. 1989. Chemical and isotopic systematics of oceanic basalts: implications for mantle composition and processes. Geological Society,

London, Special Publications 42(1): 313-345.

Suvansavate, A. 1986. Geological and mineralogical studies of the cassiterite-sulfide ore deposit at the Takua Pit Thong mine, Changwat Ratchaburi. Master's Thesis. Department of Geology, Graduate School, Chulalongkorn University.

Taylor, R. G. 1979. Geology of tin deposits. vol. 11. Developments in economic geology. Amsterdam: Elsevier Scientific.

The Industrial Technology Research Institute. 2016. 2016 Report on Global Tin Resources & Reserves. Hertfordshire, UK: The Industrial Technology Research Institute.

Ueno, K. 2003. The Permian fusulinoidean faunas of the Sibumasu and Baoshan blocks: their implications for the paleogeographic and paleoclimatologic reconstruction of the Cimmerian Continent. Palaeogeography, Palaeoclimatology, Palaeoecology 193(1): 1-24.

Ueno, K., and Charoentitirat, T. 2011. Carboniferous and Permian. In M. F. Ridd, A. J. Barber, and M. J. Crow (eds.), The Geology of Thailand, pp. 71-136. London: Geological Society.

Ueno, K., and Hisada, K. 1999. Closure of the Paleo-Tethys caused by the collision of Indochina and Sibumasu. Chikyu Monthly 21: 832-839. [in Japanese]

Varlamoff, N. 1975. Classification des gisements d'étain. Bruxelles: Koninklijke Academie voor Overzeese Wetenschappen.

Wang, C., Deng, J., Carranza, E. J., and Santosh, M. 2014. Tin metallogenesis associated with granitoids in the southwestern Sanjiang Tethyan Domain: Nature, deposit types, and tectonic setting. Gondwana Research 26: 576-593.

Wang, H., Liu, Y., Zhao, J., Hu, S., Wang, Y., Liu, C., and Zhang, Y. 2015. A Simple Digestion Method with a Lefort Aqua Regia Solution for Diatom Extraction. Journal of Forensic Sciences 60: S227-S230.

Wang, X. D., Lin, W., Shen, S.-Z., Chaodumrong, P., Shi, G. R., Wang, X.-j., and Wang, Q.-l. 2013. Early Permian rugose coral Cyathaxonia faunas from the Sibumasu Terrane (Southeast Asia) and the southern Sydney Basin (Southeast Australia): Paleontology and paleobiogeography. Gondwana Research 24(1): 185-191.

Waterhouse, J. B. 1982. An early Permian cool-water fauna from pebbly mudstones in

south Thailand. Geological Magazine 119(4): 337-354.

Wilson, M. 1989. Igneous Petrogenesis. Dordrecht: Springer Netherlands.

Wongwanich, T.   1990.   Lithostratigraphy, sedimentology and diagenesis of the Ordovician carbonates, Southern Thailand. Doctoral dissertation. University of Tasmania.

Wongwanich, T., Tansathien, W., Leevongcharoen, S., Paengkaew, W., Thiamwong, P., Charoenmit, J., and Saengsrichan, W. 2002. The Lower Paleozoic rocks of Thailand. In N. Montajit (ed.), Proceedings of the Symposium on Geology of Thailand, pp. 16-21. Department of Mineral Resouces, Ministry of Natural Resources and Environment.

Yu, S. Y., Li, K. Q., Shi, Y. P., and Zhang, H. H. 2003. A study on the granodiorite in the middle part of Lincang granite batholith. Yunnan Geology 22: 426-442. [in Chinese]
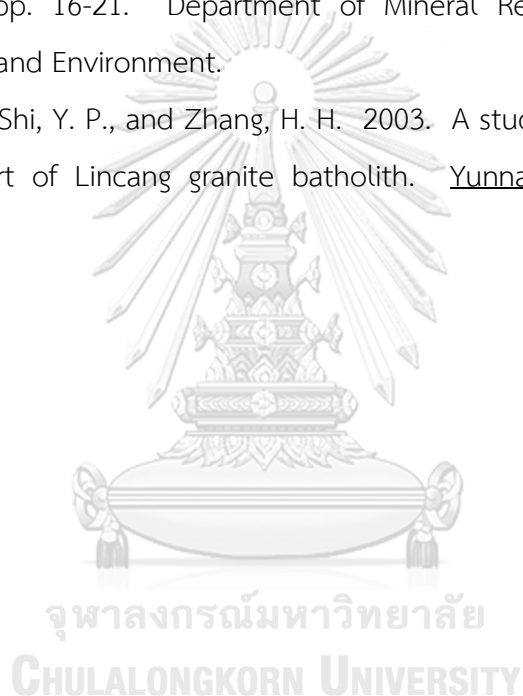
APPENDIX

SAMPLE SPECIMENS

Figure 38 Sample PL2-5-1 from Pilok area, representing biotite granite, one of porphyritic granite
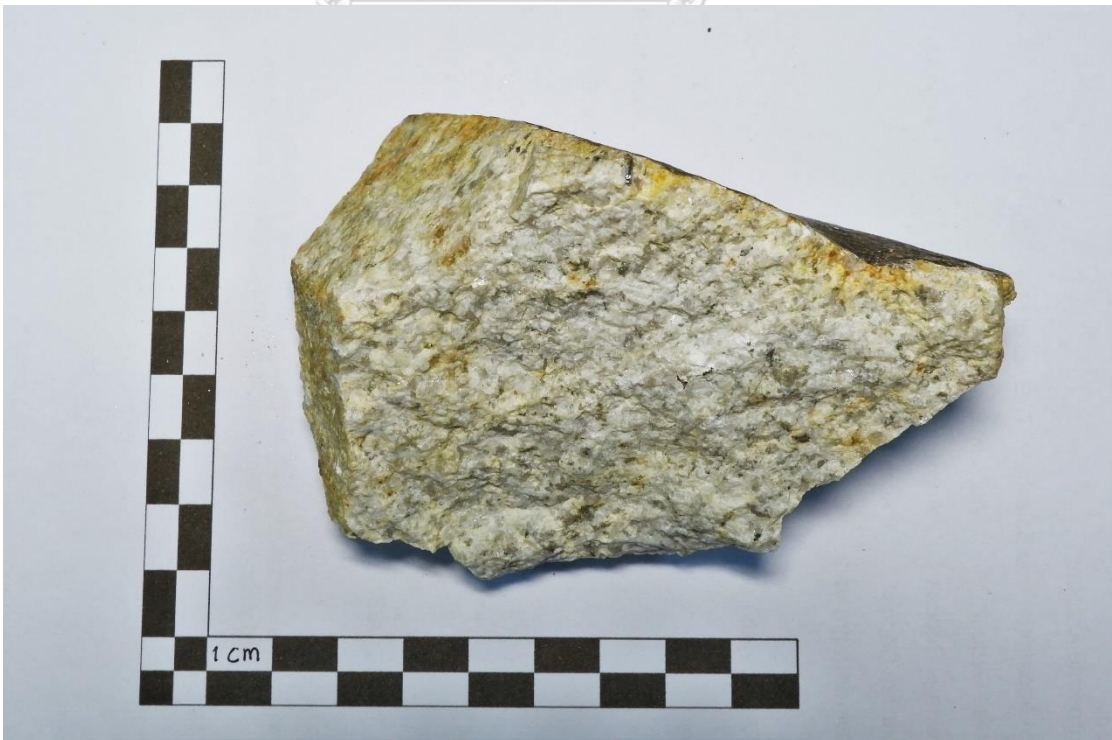

Figure 39 Sample PL3-1-3 from Pilok area, representing equigranular granite

Figure 40 Sample PL4-2-2 from Pilok area, representing tourmaline granite, one of equigranular granite

Figure 41 Sample TK1-1-5 from Takua Pit Thong, representing biotite granite, one of porphyritic granite

Figure 42 Sample TK1-1-5 from Takua Pit Thong area, representing equigranular granite

Figure 43 Sample TK4-1-4, representing tourmaline-biotite granite, one of equigranular granite

Figure 44   Sample TK2-2-1 from Takua Pit Thong area, representing greisen, one of altered granitic rock

VITA

NAME	Karn Phountong
DATE OF BIRTH	14 October 1994
PLACE OF BIRTH	Bangkok, Thailand
INSTITUTIONS ATTENDED	2020 Master of Science, Chulalongkorn University
	2017 Bachelor of Science, Chulalongkorn University
	2013 High School, Triamudomsuksa Pattanakarn School
	2007 Primary School, Somapanussorn School
HOME ADDRESS	68 Soi Romklao 19/1 Romklao Rd. Khlongsamprawet Ladkrabang Bangkok 10520
PUBLICATION	Phountong, K., Salam, A., and Manaka, T. 2020. Petrochemistry of granite from Takua Pit Thong area, Ratchaburi, Thailand. Bulletin of Earth Sciences of Thailand 11, 1: xx-xx
	Chabangborn, A., Punwong, P., Phountong, K., Nudnara, W., Yoojam, N., Sainakum, A., Won-In, K., and Sompongchaiyakul, P. 2020. Environmental changes on the west coast of the Gulf of Thailand during the 8.2 ka event. Quaternary International 536: 103-113.
AWARD RECEIVED	2019 Short stay program, ICREMER, Akita University
	2018 Outstanding graduate student award nomination
	2018 Graduate School Thesis Grant, Chulalongkorn University
	2017 Full tuition scholarship from Faculty of Science, Chulalongkorn University
	2015 Thailand Society of Petroleum Scholarship program
	2013 High School Attraction Campaign Program (HSAC) PTTEP